FINAL REPORT

NASA Grant NSG-9051

Title: Electron Microprobe Study of Lunar and Planetary Zoned Plagioclase Feldspars;

Submitted By: Dr. Robert K. Smith
Principal Investigator
University of Southern Colorado
Pueblo, Colorado 81001

To: Dr. Gary E. Lofgren
NASA Technical Officer
Johnson Space Center
Houston, Texas 77058

Grant Period: February 1977 - September 1982

Date: April 12, 1982

AN ANALYTICAL AND EXPERIMENTAL STUDY OF ZONING IN PLAGIOCLASE

Robert K. Smith
Department of Geosciences, University of Southern Colorado
Pueblo, Colorado 81001

and

Gary E. Lofgren
Geology Branch, SN6, NASA Johnson Space Center
Houston, Texas 77058

INTRODUCTION

Plagioclase in plutonic and volcanic rocks is usually compositionally zoned. This zoning may be simple normal zoning, i.e., an An-rich core which then grades continuously and smoothly to an Ab-rich rim. Often, however, the zoning is complex. There may be abrupt discontinuities with large compositional changes (10-30 An mole %) usually in a normal sense, but sometimes with reversed trends (going outward from the core the crystal becomes increasingly An-rich). There may be fine scale (a few microns) oscillations in compositions superimposed on a normal, reverse, or constant compositional trend. Finally, there may be compositional differences between different crystallographically defined sectors of the crystal which have compositional boundaries that resemble an hour glass (sector zoning). It is not unusual for all but the sector zoning to be present in a single crystal.

All of the compositional variations are caused by physio-chemical changes which affect the magma in which these crystals grow and are a record of those changes. If we can interpret those changes, much of the history of the enclosing magma body would be revealed. Attempts to understand the zoning have taken several forms. Theoretical models, especially for oscillatory zoning, are numerous. Analytical studies of the zoning profiles of individual crystals are surprisingly few. Experimental studies aimed at reproducing zoning are even fewer. Accordingly, our current understanding of plagioclase zoning is unsatisfactory. It is the primary purpose of this study to provide additional analytical data on the zoning profiles of individual crystals from a variety of different composition magmas. Data are also presented on some experimentally grown

crystals. The analytical data will then be compared to existing models. Emphasis will be placed on discontinuous or stepped and oscillatory zoning. Data on a few experimentally-grown, sector-zoned crystals will also be presented. Normal and/or reverse zoning are observed in most of the crystals studied and will be described where observed.

EXPERIMENTAL AND ANALYTICAL METHODS

The electron microprobe analyses for Na, K, and Ca were carried out on an ARL-EMX-SM electron microprobe at the NASA Johnson Space Center, Houston, Texas. An electron beam of approximately 1 μm in diameter was used with an acceleration potential of 15 Kv and a sample current of 0.02 μA. Analyzed mineral standards were used. All data was collected using 2 μm step scan traverses; each point was irradiated for 20 seconds. Six element analyses were completed using a M.A.C.-5 electron microprobe. X-ray intensities were measured using a 15 Kv acceleration potential and 0.015 μA sample current. Measured x-ray intensities were corrected for detector deadtime, background, and matrix effects using a Bence-Albee correction technique with alpha factors by Albee & Ray (1970). Mineral standards were used throughout.

The experimentally grown crystals analyzed in this study are previously described in Lofgren (1974a, b; 1980). The growth parameters are given in Table 1, and include the initial melt composition, growth temperature, cooling rate, and growth rate data where available.

ELECTRON MICROPROBE ANALYSES OF ZONED PLAGIOCLASE

During this investigation, 32 zoned plagioclase crystals were

analyzed by means of 60 step-scan traverses. Of the plagioclase crystals analyzed, 10 (18 step-scan traverses) were experimentally grown and the remainder were from a variety of rocks ranging in composition from basalt to rhyodacite. The composition of natural rock samples is listed in Table 2.

Naturally grown plagioclase crystals show extensive variations in zoning patterns and many of these zoning features have been reproduced experimentally (Lofgren, 1980). Continuous normal zoning is the most common type of zoning. There are many variations in zoning pattern superimposed on a normal zoning trend; of these, two styles of zoning seem to dominate: (1) discontinuous and (2) oscillatory. Discontinuous zoning consists of sharply-defined concentric zones each usually more An poor than the previous zone. Electron microprobe analysis of compositional variations between discontinuous zones show them to typically range from 5 to 20 An mole %. Chemical variations within each discontinuous zone can show either a reverse or normal trend. Typical oscillatory zoning shows a sharp increase in An content followed by a more gradual decrease until the next oscillation. Oscillations also show a more symmetrical An variation with a gradual increase to the center of the zone on either side. Typically, oscillatory zoning compositional variations range from 2 to 25 An mole %. Both discontinuous and oscillatory zoning are often found in the same crystal. Sector zoning is rare in natural samples and none are studied here. Sector zoning has been observed in experimentally grown plagioclase and analyses show distinct compositional differences between sectors.

Discontinuous Zoning

A typical discontinuously zoned plagioclase phenocryst (M-714)

from a fresh aa basalt from Pacaya Volcano in Guatemala (Eichelberger et al., 1973) is shown in Fig. 1. This crystal has four sharply-defined, concentric zones each more An poor than the previous zone. Chemical variations between each zone range from 10 to 15 An mole %. The core zone (zone 1) has a constant to slightly reversed chemical zoning trend averaging An 88 with minor oscillations between 2 and 4 An mole %. Zone 2 shows an initial modest reverse zoning trend followed by an overall normal zoning trend from An 77 to An 64 with superimposed oscillatory zoning consisting of differences between 2 and 4 An mole %. The initial reverse zoning trend could be considered as part of the first oscillation. Zone 3 shows both prominent reverse and normal zoning trends. The reverse zoning trend occurs between 125 μm and 100 μm with the normal zoning trend between 100 μm and 60 μm. Superimposed on this combined reverse and normal zoning pattern are minor oscillations with differences as much as 6 mole % An. The outer most zone (zone 4) shows an overall normal zoning trend with superimposed oscillations up to 7 An mole %. The reverse zoning trends observed in zones 2 and 3 are present in most of the discontinuously zoned plagioclase phenocrysts in M-714. The reverse zoning has a range of 4 to 15 An mole %.

Traverses from discontinuously zoned plagioclase crystals in a hornblende-biotite dacite (M-513) from Cactus Mountain, California are shown in Fig. 2. Two different crystals from the same thin section, approximately 1 cm apart, consist of three concentric zones each more An poor than the previous zone. As previously observed in the Pacaya basalt, the discontinuous zoning shows both reverse and normal zoning trends with superimposed oscillations. The discontinuous zones in Fig. 2 show a good correlation between

crystals; both the number of discontinuous zones and the chemical composition of each zone can be correlated. In contrast, the fine oscillations cannot be correlated. Comparison of traverses T-1 (Fig. 2A) and T-5 (Fig. 2B) show reverse zoning trends in the core zones which culminate at a composition of An 68 and An 67 respectively. A sharply defined, compositional drop occurs between zones 1 and 2 in both crystals culminating in a plateau at a composition of An 57 and An 52 for traverses T-1 and T-5 respectively. Within zone 2 each microprobe traverse shows a slight reverse trend and then a normal trend before the next discontinuous step to zone 3. In both crystals the onset of zone 3 is marked by a change in composition to less than An 40 which is followed by a reverse trend which changes to a normal trend near the edges of the crystals. Traverse T-1, however, shows more compositional variation in zone 3 than T-5.

An experimentally grown, discontinuously zoned plagioclase feldspar crystal is shown in Fig. 3 (see Lofgren, 1974b, Fig. 1B). This crystal consists of a sequence of four sharply-defined, concentric zones each more An poor than the previous zone enclosing a large core zone. The discontinuous zones were produced experimentally by dropping the temperature below the liquidus producing a significant degree of supercooling (Lofgren, 1974b). The variation in An content between each zone ranges between 11 to 26 mole %. Immediately following each rapid change in composition there is a reverse zoning trend that continues until the next discontinuous step. The temperature was held constant after the sudden change so the reverse zoning developed at constant temperature. The reverse zoning has a range of 3 to 17 An mole % with the maximum amount noted in zones 2 and 3. The magnitude of the compositional

reverse zoning is least pronounced in the core and the outer most zone.

Microprobe traverses across two additional discontinuously zoned plagioclase crystals grown from melts of different composition are shown in Fig. 4, Table 1 (see Lofgren, 1974b, Figs. 1A, 1D). In each crystal, as previously noted in Fig. 3, immediately following each discontinuously produced zone there is a continuous reverse zoning trend. Again, as in Fig. 3, the core and outer most zones, show the least reverse zoning and in Fig. 4B, the outer zone is homogeneous.

Oscillatory Zoning

Compositional data on oscillatory zoned plagioclase determined by optical methods are few (Homma, 1932; Phemister, 1934, 1945; Larsen, et al., 1938; Leedal, 1952; Carr, 1954; Panov, 1968; Wiebe, 1968); and compositional data determined by electron microprobe are even fewer (Härme & Siivola, 1966; Klusman, 1972; Subbarao, et al., 1972; Pringle, Trembath & Pajari, 1974; Sibley, et al., 1976). We will, therefore, present additional electron microprobe data on oscillatory zoning trends associated with normal zoning, reverse zoning and as already noted, discontinuous zoning in both natural and experimentally grown plagioclase crystals.

An oscillatory zoned plagioclase phenocryst in a basalt from Chile with an overall normal zoning trend is shown in Fig. 5. In this example, oscillations are on the order of 1 to 2 An mole % (Fig. 5A). The overall compositional variation for traverse T-1, Fig. 5A, is from An 59 to An 55 over a distance of 50 μm.

Approximately 120 μm distance from the above microprobe traverse a second analysis was run on the same crystal, traverse T-6, Fig. 5B. This traverse shows the same normal, oscillatory zoning trend as

traverse T-1. However, major compositional differences exist between the two traverses. Traverse T-6 shows an overall compositional variation from An 80 to An 57, and compared to traverse T-1 has greater An mole % variations throughout. Additional differences include a reverse zoning trend and discontinuous zones. The reverse zoning occurs from 74 to 64 μm with an An mole % increase from An 73 to An 80. The discontinuous zone occurs at 64 μm with a sharp decrease in composition from An 80 to An 70. This sharp decrease in An mole % is immediately followed by a second reverse zoning trend from An 70 to An 72. A second sharp decrease in composition from An 72 to An 64 denotes a second narrow discontinuous zone. This decrease is again followed by an increase from An 64 to An 78. At this point, a normal zoning trend begins between 40 μm and 10 μm. Such chemical variations occurring laterally along the same optically observable zone are most likely the result of local variations within the magma and which are represented by crystal-liquid boundary kinetics. However, such compositional differences may also be explained by the combination of crystal-liquid boundary kinetics and growth relationships between different crystal faces.

A zoned plagioclase crystal (M-736) from a latite (trachyandesite) from the San Juan Mountains, Colorado is shown in Fig. 6. This crystal has a nearly homogeneous core (An 39) enclosed by an outer region of oscillatory zoning which is superimposed on a discontinuous step preceded and followed by reverse zoning trends. A slight decrease in the An mole % at 75 μm marks the boundary between the core region and the oscillatory zoned region. The first reverse zoning trend ranges from An 38 to An 45 and extends from 75 μm to 105 μm where the An mole % levels off. The discontinuous

zone occurs at 130 μm with an An mole % drop of nearly 10%. From this point (130 μm) another reverse zoning trend with superimposed oscillatory zoning begins and continues to the 205 μm mark where a normal zoning trend begins. The crystal rim, however, shows another reverse trend with a 7 An mole % increase at 245 μm.

In some of the crystals analyzed, oscillatory zoning is superimposed on what would be an otherwise homogeneous crystal. Such crystals commonly have both large and small scale oscillations. The large scale oscillations stand out and are of nearly constant composition. Three examples are described below.

The first example is a plagioclase crystal (Fig. 7A, M-229B) in a trachyte from near the Hoover Dam, Arizona. It displays rhythmic oscillations superimposed on an average chemical background of An 32. Each successive rhythmic oscillation, at 50, 150, and 195 μm respectively, is followed by a normal and more gradual decrease in the An content compared to the rather sharp increase in An content preceding each oscillation. There is a slight (approximately 2 An mole %) drop between successive peak heights from the crystal interior toward the rim. Relatively smaller oscillations from 2 to 6 An mole % occur between the three major rhythmic spikes.

A second example in a basalt from Chile (M-598) is shown in Fig. 7B. This oscillatory zoned plagioclase phenocryst exhibits rhythmic oscillations, in this case, all peaking near An 76 on a nearly constant chemical background of An 66. Zone 1 starts with a composition of An 64, shows a reverse zoning trend from An 64 to An 70 between 0 and 10 μm, followed by a normal zoning trend with minor oscillations between 10 and 30 μm. Zone 2 begins with a sharp increase in An mole % from 66 to 76, which marks the beginning of a

rhythmically zoned region consisting of five separate peak spikes all of approximately An 76. After the last rhythmic oscillation spike at 88 μm, there is a slight reverse zoning trend which marks the beginning of zone 3. Zone 3 is characterized by a normal trend after the initial reverse trend with only minor oscillations in An mole %. The outer most edge of zone 3 shows a sharp compositional drop from approximately An 60 to An 45.

The third example is shown in Fig. 8, and is also in a basalt from Chile (M-600). This crystal has a normally zoned central core, An 50 to An 30, with an outer zone containing four rhythmic oscillations. The rhythmic oscillations occur on a relatively constant chemical background with a mean of approximately An 35. The numerous microprobe traverses (Fig. 8A) completed on this phenocryst, provides an excellent opportunity to correlate the four major rhythmic oscillations on two crystal faces. Of the four separate rhythmic spikes, three are within 5 to 7 An mole % of one another (Figs. 8B, C, D); i.e., all three lie between An 48 and An 55. The fourth and outermost spike has a composition of An 43. Between these four An-rich, rhythmic oscillations on face (100) (Fig. 8A) there are minor oscillations with compositions ranging between An 38 and An 30. These minor oscillations on face (100) show excellent correlation between traverses T-1 and T-5 (Fig. 8B, C). However, traverse T-7 (Fig. 8D) normal to face (001) shows a complete lack of minor oscillations between the four major spikes. Such minor chemical variations occurring on the different crystal faces may be due to crystal-liquid boundary kinetics and the rate of crystal growth of these faces or due to the very small area between major oscillations on face (001) any minor chemical variations

that may be present are not recorded because of the microprobe beam spot size.

Zoned plagioclase crystals displaying oscillatory zoning have also been grown experimentally in controlled cooling experiments (Lofgren, 1980). An experimentally grown plagioclase crystal displaying oscillatory zoning is shown in Fig. 9 (run conditions are given in Table 1). The oscillatory zoning is very fine with small compositional variations ranging from 1 to 2 An mole %. Such small compositional variations have been observed both optically and by the electron microprobe and are superimposed on a normal zoning trend which is initially flat with rapidly decreasing An content toward the rim (Fig. 9). Lofgren (1980) has also noted that the oscillations produced experimentally are best developed in the An 40-60 bulk compositional range.

Sector Zoning

Sector zoned plagioclase crystals have been grown experimentally (Fig. 10). Microprobe traverses on two crystals are shown. In Figs. 10A and B, traverses at right angles show the normal zoning trend in each sector. The sector boundaries are evident because of differences in extinction between the sectors. These differences in extinction are caused by differences in composition. It can be seen in the traverses that the core part of the (010) sector (Fig. 10A) is more calcic than the core part of the (001) sector. The compositional difference is maintained along the sector boundary. This feature is better illustrated in Figs. 10C, D. The traverse (Fig. 10C) cuts across two sector boundaries. The compositional profile (Fig. 10D) shows the sharp compositional disparity between sectors. The (001) sector is about An 50 while the (010)

sector is about An 60 at the sector boundary and zoned normally to An 45 to 48 at the edge of the crystal. A similar example is shown in Lofgren (1980, Fig. 14A, B).

Sector zoned plagioclase is rare in nature, but have been described and analyzed by Bryan (1974) in basalts from the ocean floor. He found that similar to the experiments, the (010) sectors were more An-rich than the (001) sectors. He also found that FeO and MgO were enriched in the (010) sector. Individual sectors were normally zoned.

EVALUATION OF THE MICROPROBE DATA

A major concern of the analytical method is how precise are 3 element (Na, K, Ca) analysis with a 1 μm beam diameter using 2 μm step scan traverses. Three approaches have been used to evaluate the quality of the data: microscopic (visual), six element electron microprobe analyses on selected crystals using a different microprobe, and a statistical evaluation.

In the first method, plagioclase compositional variations are determined with microscopic measurement of optical extinction and compared with microprobe data. Several of the zoned plagioclase crystals, which have the proper crystallographic orientation in thin section, were selected for measurement using Schuster's method (Schuster, 1880; Köhler, 1942). Fig. 11 and Table 3 show the direct comparison between the microscopic and microprobe analyses conducted on two discontinuously zoned plagioclase crystals. The data in Table 3 show the excellent chemical correlation between the two methods. All abrupt compositional changes are quite evident optically as well as on the microprobe traverses.

The second method involved more complete, six element analyses (Na, K, Ca, Al, Si, and Fe) for four of the crystals analyzed for three elements, two natural occurring and two experimentally grown. An electron beam of anproximately 1 μm in diameter was used with an acceleration voltage of 15 Kv and a sample current of .015 μA. For each crystal the original 2 μm step scan traverse was located and multiple spot analyses performed along the traverse. Each individual spot analysis was then plotted directly on the original 2 μm step scan traverse as shown in Fig. 12. In all instances less than a 2 An mole % difference is noted between the three and six element microprobe analyses.

This close chemical similarity, confirmed by two separate and independent methods, implies that three element analyses combined with a 2 μm step scan traverse are sufficiently accurate to study zoned plagioclase phenocrysts.

A third major concern is the compositional significance of the very small, but sharp, microprobe compositional oscillations (on the order of 1 to 2 An mole %) as noted along most of the microprobe traverses. Whether such minor oscillations are evident optically is primarily a function of the crystallographic orientation of the crystal (compare Figs. 3 and 5). It is important, however, to know whether these small oscillations reflect actual chemical variations within the crystal, i.e., what An mole % change should be considered significant. In order to make this judgment, the accuracy of x-ray photon counting measurements as they pertain to microprobe analyses of zoned plagioclases were analyzed statistically.

A statistical analysis procedure for x-ray counting measurements must address two problems. X-ray photons are randomly emitted from

the irradiated sample, causing the x-ray intensity to fluctuate in a statistical manner above and below a mean value. If there were no beam damage to the sample surface, the longer the sample is exposed to the radiation source, the more accurate the calculated mean intensity will be, for every quadrupling of the count time. However, because the electron beam does alter the surface characteristics of the sample during a scan, this prevents the rechecking of the traverse a second time. This inability to remeasure the exact traverse eliminates the possibility of computing the mean and standard deviation of the microprobe traverse composition by normal statistical methods. Therefore, to have a valid statistical analysis between microprobe traverses, these two problems must be accounted for.

The inability to remeasure the exact microprobe traverse can be overcome by using multiple microprobe traverses across the same zones in the same plagioclase crystal.

To test the accuracy of the statistical approach a zoned plagioclase crystal had to be chosen for which numerous electron microprobe traverses had been conducted and for which small microprobe compositional oscillations, to be checked statistically, could be observed microscopically and therefore correlated from traverse to traverse. The zoned plagioclase crystal shown in Fig. 8A was chosen because it met the criteria listed above. All microprobe traverses and the location of each are shown in Fig. 8A. In order to test the validity of the small compositional oscillations in this particular zoned plagioclase crystal, a region bounded by the two major zonal spikes correlated by dashed lines in Fig. 13 was chosen. Four separate

microprobe traverses (as shown in Fig. 13) were chosen for the statistical analysis. Because microprobe traverses T-4 and T-5 were run separately under different beam currents compared with traverses T-1 and T-2, normal x-ray photon counts for Ca, Na, and K from each of these four regions could not be used for statistical analysis. However, the computed An mole % from the raw data can be used. Therefore, Table 4 lists all An mole % from each of the four traverses used for various statistical analyses. Also listed in Table 4 are the means and standard deviations for each population of the four microprobe traverses, as well as the mean and standard deviation for the total population of traverses T-1, T-2, T-4, and T-5. Standard deviations or Z scores for the three separate and visually correlatable minor oscillations are also listed in Table 4 (compare Fig. 13 noting the exact three zones under question). Because the sample size was so small the null hypothesis was also tested using the conservative t test. The null hypothesis, in this case, states that the mean of each zone is equal to the mean of the total population observed. All t scores for the mean of zones 1, 2, and 3 are listed in Table 4.

The significance one usually associates with normal statistical x-ray measurement accuracy is as follows: (1) if differences exceed three or more standard deviations, this difference is considered significant at the 95% or better confidence level, (2) if the difference is exceeded by two standard deviations or more, this difference is considered significant at the 90% confidence level, and (3) if the difference does not exceed one standard deviation, the difference is considered non-significant. From an examination of

Table 4, it can be seen that standard deviation differences from -0.66 to -1.63 (t = -2.13), -0.55 to 0.11 (t = -0.13), and -1.61 to -2.52 (t = -3.84) exist for zones 1, 2, and 3 respectively. Under normal circumstances zones 1 and 3 would be considered significant (at the 90% and 95% confidence level respectively) while zone 2 would be considered non-significant. However, because correlation between these minor An variations can be made easily with the microscope for zone 2, one must re-evaluate the significance of the standard deviations for zone 2 (see Table 4).

Hypothesis testing using the non-parametric sign test (i.e., no assumptions about the population are made) was also conducted on the An mole % data listed in Table 4. In this test one only looks at patterns; i.e., positive or negative values (slopes and not the magnitude between An mole % differences). The sign test for zone 1 shows a small probability (6%) that there is no pattern of differences; telling us that we can expect a negative and a positive slope on either side of our microscopically observable and correlatable zone. In other words there is a "valley" that can be traced for zone 1 from traverse to traverse. The 94% confidence level is all that can be expected based on the present sample size. Sign tests for zones 2 and 3 yield the exact same results.

Therefore, based on the standard deviation differences (Z scores), t tests, and sign tests (Table 4), combined with the visual correlation of those minor zones labeled 1, 2, and 3 in Fig. 13, minor An chemical variations from 1 to 2 An mole % are considered to be significant in the present study.

PLAGIOCLASE ZONING MODELS

In this discussion of theoretical models for plagioclase zoning in relation to the data presented in this paper, we will not attempt a thorough review of all models, nor even an in-depth description of specific models. We will outline the salient features of the pertinent models. The full flavor of each model can be obtained only from the original papers (see also Smith, 1974, pgs. 212-224). Models exist for normal, reverse, discontinuous (stepped), oscillatory and sector zoning. Models for normal and discontinuous zoning are straight forward; those for sector and reverse zoning are complex, but reasonably well understood; and those for oscillatory zoning, though more numerous, are the least satisfactory.

Normal Zoning and Unzoned Crystals

Normal zoning is most simply defined as a change of chemical composition from a more calcic core to a less calcic rim of a plagioclase crystal. The pattern can be simple: a smooth curve from core to rim, or complex: containing all or most of the different varieties of plagioclase zoning. It is the simple, smooth profile which we are discussing here. Klusman (1972) has presented a model where Ca partitioning between liquid and solid follows a logarithmic distribution law with an exponential factor which varies as a function of liquid composition. The resulting zoning profile is initially flat (of constant composition) over approximately the inner 2/3 of the crystal followed by a rapid decrease in CaO content (increase in Na_2O content) towards the edge of the crystal.

Plagioclase crystals grown in slowly cooled experiments (~2^{o}C/hr) have such profiles (Figs. 9, 10A). Plagioclase crystals grown in

more rapidly cooled experiments have more linear profiles (Fig. 10B, 10D). Lofgren (1973, 1980, Fig. 12) shows a series of normal zoning compositional profiles from crystals grown at different cooling rates. With increasing cooling rate the profile is more linear and more restricted in compositional range. If grown sufficiently rapidly, the resulting microlitic plagioclase will be nearly homogeneous and have grown at a composition not greatly dissimilar from that which uses all the feldspar components in the melt, i.e., the equilibrium composition.

The Klusman model for logarithmic distribution thus applies to crystals grown under near interface equilibrium conditions. Evans & Moore (1968) reported a more restricted range of plagioclase zoning (An_{70} to An_{42}) in crystals from the chilled margin of a lava lake in Hawaii compared to crystals from the center of the lava lake ($An_{77}Or_1$ to $Or_{64}Ab_{33}An_3$). These data are consistent with the experimental results and show the importance of kinetic control of plagioclase composition. In the more rapidly cooled lava, the plagioclase nucleates at a lower temperature and thus has a less An-rich core (An_{70} compared to An_{77}). The faster cooling rate also inhibits continued growth (An_{42} compared to $Or_{64}Ab_{33}An_3$ for a rim composition). In the more slowly cooled lava plagioclase can nucleate at a higher An composition and continues to grow to lower temperatures and thus shows a larger zoning range. Lofgren & Gooley (1977) show examples of slowly cooled experiments which produced feldspars similar to those described by Evans & Moore from the center of the lava lake.

It is ironic that plagioclases which have the equilibrium composition are only grown at rapid cooling rates and are usually

microlites. Large homogeneous plagioclase crystals in an igneous rock are more of an enigma. When they exist, they are usually very calcic and most likely represent growth of a small fraction of the feldspar from the melt, i.e., the flat portion of the logarithmic curve of Klusman. The important question is why the zoned outer portion of the crystal did not develop. There are several possible answers. Most commonly the outer zoned portion is there but very thin, 10 to 20 microns. This might happen if there was the rapid crystallization of groundmass plagioclase restricting the amount of material available to the large crystals. If there is absolutely no zoning, growth must have been arrested by rapid cooling or some other mechanism.

Discontinuous Zoning and Reverse Zoning

Discontinuous zoning has perhaps the most obvious origin of any of the kinds of plagioclase zoning. It was recognized early that a rapid change of temperature or pressure (combined with loss of volatiles) could cause this type of zoning. It was also recognized that a change of pressure is more likely to happen fast enough to cause the observed sharp discontinuity (Phemister, 1934) than a change in temperature. Discontinuous zoning has been reproduced experimentally by Lofgren (1974b) and some of the experiments described in that earlier paper are analyzed here. The discontinuities are produced readily by rapid changes of temperature. The magnitude of the compositional break is a direct function of the magnitude of the temperature change. For purposes of experimentally studying the zoning, the crystal doesn't know how the increased degree of supercooling or supersaturation is induced; it merely responds to an increased driving force for crystallization. In experiments,

temperature is the easiest variable to change. In nature, a sudden pressure change would produce a similar discontinuity followed by renewed growth at either a lower or higher An content depending on water content (Wiebe, 1968). Such discontinuties might also be produced in a rapidly ascending magma, but again the accompanying pressure change would cause the discontinuity.

In the experiments, each temperature change was followed by an isothermal period of crystallization. The crystal grown during this isothermal period is usually reversely zoned or occasionally unzoned, never normally zoned. In the magma which experiences a sudden pressure change, there would most likely be a similar period of isothermal growth once the pressure is again constant. Similarily the natural plagioclase crystals, as demonstrated earlier in this paper, show a reverse zoning trend following most of the sharp discontinuities.

Lofgren (1974b) explained the origin of this pattern of reverse zoning as a kinetically controlled response to a sudden change in either the degree of supercooling or the degree of supersaturation. If the rapidly induced degree of supercooling is sufficiently large there is a strong probability that continued growth will be at a composition more sodic than the composition predicted by the position of the solidus at that temperature. The reverse zoning trend is then the result of the system's attempt to approach the equilibrium condition as continued growth reduces the degree of supercooling in the system. It is easily seen that depending on the magnitude of the rapidly induced degree of supercooling the magnitude of the reverse zoning will vary. In addition, if the system is cooling at a significant rate when the sudden change occurs, the normal zoning which results from

cooling would reduce, eliminate, or even cause a normal zoning trend. In the experiments any heat of crystallization is eliminated in the controlled environment, in nature it would add to the magnitude of the reverse zoning. Any significant elevation of temperature, however, would result in resorption of the already crystallized material and would be apparent in the crystal.

Sector Zoning

The models for sector zoning have been developed primarily for clinopyroxene, but have been applied to other minerals such as staurolite, quartz, andalusite, and epidote. Only Dowty (1976) mentions plagioclase. The models are based on an interplay of structural control and growth rate in a disequilibrium growth environment. Some workers emphasize the importance of structural control (Hollister & Bence, 1967; Hollister, 1970; Nakamura, 1973; Dowty, 1976) and others emphasize the differences in growth rates of different crystal faces in the disequilibrium environment (Wass, 1973; Leung, 1974; Downes, 1973). The most successful model appears to be that of Dowty (1976) which is based primarily on the nature and number of the crystal sites available on the different faces during growth. Impurities will be adsorbed in these sites and then trapped as they are covered by the next layer of atoms. For the impurities to be trapped the growth must be sufficiently rapid to prevent the adsorbed cations from leaving these sites they are temporarily occupying.

For the sector zoning observed in the experiments where the faster growing (001) sector is more Na-rich and the slower growing (010) sector is more Ca-rich, a model based on faster growth rates incorporating more impurity (in this case Na) would appear to be

sufficient. This model would not explain, however, the preferential incorporation of FeO and MgO in the (010) sector observed by Bryan (1974) or the preferential incorporation of trace elements in the (010) sector observed by Shimazu (1981). The model of Dowty (1976) has four 4/9 sites on the surface of least bonding for the (010) face while the surface of least bonding on (001) exposes only two 4/9 sites. The 4/9 sites would prefer Ca, Mg, Fe and other trace elements to sodium even at the slower growth rate extant on the (010) face relative to (001). The magnitude of the growth rate disparity between the faces and the variation of the absolute growth rate on (010) would affect the magnitude of the compositional differences between the faces. In the experiments, crystals grown at cooling rates near 1°C/hr showed little, if any, compositional variation across the sector boundary in the few cases where a sector boundary is present. Crystals grown at faster cooling rates showed a larger compositional disparity between sectors (Fig. 10C, D; Lofgren, 1980).

The rarity of sector zoned plagioclase (Bryan, 1974) may well be explained by the relatively rapid cooling rate (1°C/hr is a relatively rapid cooling rate except in lava flows) required to produce sector zoning.

Oscillatory Zoning

Oscillatory zoning consisting of successive and at times rhythmic compositional variations from core to margin of a plagioclase crystal has been a subject of discussion for many years (e.g., Harloff, 1927; Bowen, 1928; Homma, 1932; Phemister, 1934; Hills, 1936; Carr, 1954; Vance, 1962; Bottinga et al., 1966; Sibley et al., 1976; Haase et al., 1980; Allegre et al., 1981). Theories for the origin of oscillatory zoning can be divided into two main groups.

One group of theories is based on repeated changes in crystal-liquid equilibrium as a result of sudden changes of temperature, pressure, water saturation, and melt composition. For example, Bowen (1928) and Homma (1932) explain the origin of oscillatory zoning in terms of the repeated convective movement between crystals and a physico-chemical heterogeneous melt. Carr (1954) interprets oscillatory zoning in the Skaergaard as the result of cyclic pressure changes due to convective overturn. The second group of theories is based on disequilibrium growth of the crystal. The first was proposed by Harloff (1927) who suggested that oscillatory zoning forms as the result of the interplay of the crystal growth and diffusion rates. The diffusion-supersaturation theory of Hills (1936) expanded on the original concept of Harloff (1927). Subsequent authors have elaborated on this theme (e.g., Vance, 1962; Bottinga et al., 1966; and Sibley et al., 1976). Bottinga et al. (1966) present data and arguments suggesting that plagioclase crystallization is diffusion controlled at some stage during the crystallization process as postulated by Harloff (1927), but by the relative diffusion rates of Si and Al not Na and Ca. They also suggest that a finite supersaturation is necessary to initiate precipitation of a zone. Sibley et al. (1976) have suggested oscillatory zoning is the result of changes in the growth rate of the crystal and the diffusion rate of solute at the crystal-liquid boundary.

Haase et al. (1980) and Allegre et al. (1981) take a slightly different approach. Haase et al. (1980) suggest that oscillatory zoning originates from an interplay of the following factors: the growth rate is a function of the melt composition and changes in melt composition at the crystal surface created by

differences in diffusion rates of the different melt species accepted or rejected by the crystal; the nature of the melt species incorporated at the interface and their relative rate laws; and motion of the growing crystal rim. The solution to their mathematical formulation is multivalued and the oscillatory behavior presumably occurs between these values.

Allegre et al. (1981) critique the above models and find them lacking in one critical ingredient, the driving force for or an explanation of the oscillatory behavior. All the models explain a plausible single cycle of crystallization, but do not adequately account for repetition of the cycle. Allegre et al. (1981) attempt to explain the repeating cycles by postulating that for a crystal whose growth has slowed because of the changing melt composition at the interface there is a characteristic time for structural rearrangement before the growth rate can increase. They provide a mathematical formulation of the growth equation which, with the incorporation of the characteristic delay time, they claim does provide for true oscillatory behavior.

It is clear that the experimental growth of oscillatory zones in plagioclase would, at this time, aid in the evaluation of the models. If prediction of Allegre et al., is true, however, the growth rate for oscillatory zoned crystals would be very slow, perhaps too slow for laboratory experimentation. This may explain the difficulty one of the authors (GEL) has had growing oscillatory zoned crystals in the laboratory. Only in one experiment out of more than 50 attempts have oscillatory zoned plagioclase crystals been grown (Fig. 9; Lofgren, 1980). This experiment, however, was not at the slowest cooling rate attempted as the model of Allegre et al. (1981)

would suggest it should be.

The experimentally produced oscillatory zoned crystals resemble the zoning described by Gutmann (1977) in basaltic plagioclase, but does not mimic any of the oscillatory zoned crystals examined in this study. Before the oscillatory zoning mechanism and the environments in which the different styles and magnitudes of oscillatory zoning are produced can be adequately understood, the models must accurately explain the variations in magnitude and style of the oscillatory zoning.

SUMMARY

Normal and discontinuous zoning in plagioclase feldspars have been successfully reproduced experimentally. Normal zoning was produced in melts cooled over a given temperature interval. The normal zoning profile and the composition range were found to vary with the cooling rate. At slow cooling rates (~2°C/hr) the plagioclase compositional profiles shows little if any zoning until the outer portion of the crystal is reached. In this case the normal zoning profile closely follows the Klusman (1972) model for Ca partitioning between liquid and solid which varies as a function of the liquid composition. Normally zoned plagioclase crystals grown at increasingly more rapid cooling rates show that the zoning profile becomes more linear and more restricted in compositional range. In general, the faster the cooling rate, the more restricted will be the zoning interval.

Discontinuous zoning has been reproduced experimentally by rapid changes of temperature. The magnitude of the discontinuous (compositional) drop is a direct result of the magnitude of the temperature drop. Experimentally, temperature is the easiest variable to

change. However, naturally formed plagioclase crystals with discontinuous zoning is more likely to be produced by a rapid change in pressure. Discontinuous zoning observed in naturally formed plagioclases of similar size and within the same thin section shows remarkable correlation between crystals (see also Greenwood & McTaggart, 1957). Both the number of observed discontinuous zones and the chemical composition of each discontinuous zone from crystal to crystal can be correlated. Such correlation between plagioclases containing discontinuous zoning supports a mechanism of physical changes external to the magma, e.g., pressure, temperature, and water saturation.

Reverse zoning is not common in natural igneous plagioclase feldspars, but was observed in the discontinuous zoning experiments. After each rapid temperature drop a period of isothermal crystallization followed. Reverse zoning resulted during most of these periods of isothermal growth. In the natural plagioclases reverse zoning has been shown to occur after most sharp discontinuities. Here again, as in the case for discontinuous zoning, sudden pressure changes would most likely be followed by isothermal growth at constant pressure and therefore, result in the possibility of reverse zoning. One would expect therefore, reverse zoning to occur by either a sudden pressure change or a large temperature drop followed by isothermal crystallization. The reverse zoning is explained as a kinetically controlled response to a sudden change in either the degree of supercooling or the degree of supersaturation.

Sector zoning in plagioclase is also rarely seen in naturally grown feldspars; Bryan (1974) describes one of the few occurrences. Sector-zoned plagioclase crystals were not observed in the natural

rock specimens studied here, but has been observed in experimentally grown plagioclases. In both the natural and synthetic plagioclase crystals, the (001) sector is the most Na-rich and the fastest growing while the (010) sector is the most Ca-rich and the slower growing. The (010) section, however, is usually enriched in trace-elements which contradicts the simple growth rate model. Dowty (1976) appears to have the most successful hypothesis; his model is based on the nature and number of the crystal sites available on the different faces during the growth.

Oscillatory zoning consisting of successive and at times rhythmic compositional variations is common in plagioclase and has long been a topic of discussion. Two groups of theories for its origin exist. The first group is based on repeated changes in crystal-liquid equilibrium as a result of sudden changes of temperature, pressure, water saturation, and melt composition in the magma chamber. The second group is based on disequilibrium growth of the plagioclase crystal; most are variations of Harloff's (1927) diffusion-supersaturation theory. To date, all the models explain a plausible single cycle oscillation, but only that of Allegre et al. (1981) adequately accounts for repetition of the cycle.

Plagioclase crystals displaying oscillatory zoning have been produced in controlled cooling experiments. The crystals are few in number, are best developed in the An40-60 bulk compositional range, and show only very fine zones with very small compositional variations. Microprobe and optical analyses on oscillatory zoned crystals of natural and experimental plagioclase shows a complete lack of correlation between oscillatory zoning in plagioclases from crystal to crystal within a given thin section (see also Wiebe, 1968). This

lack of correlation between different oscillatory zoned plagioclases and the ability to produce oscillatory zoning experimentally suggest a formation mechanism related to the kinetics of crystal growth. So few laboratory experiments, however, have produced plagioclase crystals with oscillatory zoning that a complete understanding of the crystal growth mechanism has not been fully developed. The rarity of experimentally produced oscillatory zoning may well be because it occurs at cooling rates so slow they are difficult to reproduce in the laboratory as suggested by Allegre et al. (1981).

ACKNOWLEDGEMENTS

This work was supported by NASA grant NSG-9051. Microprobe analyses were performed at the Johnson Space Center, Houston, Texas with the assistance of Roy Brown. J. Eichelberger supplied sample (M-714) from Pacaya Volcano in Guatemala. Laboratory data were collected with the assistance of D. L. Whitley, G. X. Hernandez, M. R. Florez, J. L. Cook, L. N. Goessman, and M. K. Story. We thank Roger W. Johnson for reviews and discussion concerning all statistical analyses, however, we assume all responsibility for interpretations and conclusions reached. We also appreciate the useful comments and suggestions by Maynard Slaughter. Pat Vigil and Florence McClary typed the manuscript.

REFERENCES

Albee, A. L., & Ray, L. 1970: Correction factors for electron probe microanalysis of silicates, oxides, carbonates, phosphates, and sulfates. Anal. Chem. 42, 1409-1414.

Allegre, C. J., Provost, A., & Jaupart, C. 1981: Oscillatory zoning: A pathological case of crystal growth. Nature 294, 223-228.

Bottinga, Y., Kudo, A., & Weill, D. 1966: Some observations on oscillatory zoning and crystallization of magmatic plagioclase. Am. Min. 51, 792-806.

Bowen, N. L. 1928: The evolution of the igneous rocks. Dover Pub. Inc., New York.

Bryan, W. B. 1974: Fe-Mg relationships in sector-zoned submarine basalt plagioclase. Earth Planet. Sci. Lett. 24, 157-165.

Carr, J. M. 1954: Zoned plagioclases in layered gabbros of the Skaergaard intrusion, east Greenland. Min. Mag. 30, 367-375.

Downes, M. J. 1973: Some experimental studies on the 1971 lavas from Etna. Phil. Trans. R. Soc. Lond. A. 274, 55-62.

Dowty, E. 1976: Crystal structure and crystal growth: II. Sector zoning in minerals. Am. Min. 61, 460-469.

Eichelberger, J., McGetchin, T. R., & Francis, D. 1973: Mode of emplacement of aa basalt flows at Pacaya, Guatemala. (abstr.) EOS Trans. Am. Geophys. Un. 54, 511.

Evans, B. W., & Moore, J. G. 1968: Mineralogy as a function of depth in the prehistoric Makaopuhi tholeiitic lava lake, Hawaii. Contr. Mineral. Petrol. 17, 85-115.

Greenwood, H. J., & McTaggart, K. C. 1957: Correlation of zones in plagioclase. Am. Jour. Sci. 255, 656-666.

Gutmann, J. T. 1977: Textures and genesis of phenocrysts and megacrysts in basaltic lavas from the Pinacate volcanic field. Am. Jour. Sci. 277, 833-861.

Haase, C. S., Chadam, J., Feinn, D., & Ortaleva, P. 1980: Oscillatory zoning in plagioclase feldspar. Science 209, 272-274.

Harloff, C. 1927: Zonal structure in plagioclase. Leidsche Geol. Mededeilingen 2, 99-113.

Härme, M., & Siivola, J. 1966: Plagioclase zoning in a gabbroic dike from Alatarnio, northern Finland. Compter Rendus Soc. Geol. Finlande 38, 283-288.

Hills, E. S. 1936: Reverse and oscillatory zoning in plagioclase feldspars. Geol. Mag. 73, 49-56.

Hollister, L. S. 1970: Origin, mechanism, and consequences of compositional sector zoning in staurolite. Am. Min. 55, 742-766.

Hollister, L. S., & Bence, A. E. 1967: Staurolite, sectorial compositional variations. Science 158, 1053-1056.

Homma, F. 1932: Über das Ergebnis von Messungen an zonaren Plagioklasen aus Andesiten mit Hilfe des Universal-drehtisches. Schweiz. Min. Pet. Mitt. 12, 345-352.

Klusman, R. W. 1972: Calcium fractionation in zoned plagioclase from the Tobacco Root batholith, southwestern Montana Chem. Geol. 9, 45-56.

Köhler, A. 1942: Drehtischmessungen an Plagioklaszwillingen von Tief und Hochtemperaturoptik. Min. Pet. Mitt. 53, 159-221.

Larsen, E. S., Irving, J., Gonyer, F. A., & Larsen, E. S., 3rd 1938: Petrologic results of a study of the minerals from the Tertiary volcanic rocks of the San Juan region, Colorado. Am. Min. 23, 227-257.

Leedal, G. P. 1952: The Cluanie igneous intrusion, Inverness-Shire and Ross-Shire. Geol. Soc. Lond. Quar. Jour. 108, 35-63.

Leung, I. S. 1974: Sector zoned titanaugites: morphology, crystal chemistry and growth. Am. Min. 59, 127-138.

Lofgren, G. E. 1973: Experimental crystallization of synthetic plagioclase at prescribed cooling rates. (abstr.) EOS Trans. Am. Geophys. Un. 54, 482.

Lofgren, G. E. 1974a: An experimental study of plagioclase crystal morphology: isothermal crystallization. Am. Jour. Sci. 274, 243-273.

Lofgren, G. E. 1974b: Temperature induced zoning in synthetic plagioclase feldspar. In "The Feldspars", 362-375, W. S. MacKenzie & J. Zussman, eds. Manchester University Press. Crane, Russak, and Company, Inc., New York.

Lofgren, G. E. 1980: Experimental studies on the dynamic crystallization of silicate melts. In "Physics of Magmatic Processes", 487-551, R. B. Hargraves, ed., Princeton Univ. Press, Princeton.

Lofgren, G. E., & Gooley, R. 1977: Simultaneous crystallization of feldspar intergrowths from the melt. Am. Min. 62, 217-228.

Nakamura, Y. 1973: Origin of sector-zoning of igneous clinopyroxenes. Am. Min. 58, 986-990.

Panov, Y. N. 1968: Composition and zoning of plagioclases in granitoids of northeast Transbaykal. Trans. from Maematicheskiye Metody v Geologii, vyp 1, Minist, Geol. SSSR, VSEGEI, Leningrand, 47-61.

Phemister, J. 1934: Zoning in plagioclase feldspar. Min. Mag. 23, 541-555.

Phemister, T. C. 1945: The coast range batholith near Vancover, British Columbia. Geol. Soc. Lond. Quar. Jour. 101, 37-88.

Pringle, G. J., Trembath, L. T., & Pajari, G. J., Jr. 1974: Crystallization history of a zoned plagioclase (microprobe analysis of zoned plagioclase from Grand Manan tholeiite sheet). Min. Mag. 39, 867-877.

Schimizu, N. 1981: Trace element incorporation into growing augite phenocryst. Nature 289, 575-577.

Schuster, M. 1880: Ueber die optisch Orientierung der plagioklase. Tscherm. Min. Pet. Mitt. 3, 117-284.

Sibley, D. F., Vogel, T. A., Walker, B. M., & Byerly, G. 1976: The origin of oscillatory zoning in plagioclase: a diffusion and growth controlled model. Am. Jour. Sci. 276, 275-284.

Smith, J. V. 1974: Feldspar minerals. Vol. 2: Chemical and Textural Properties. Springer-Verlag, New York.

Subbarao, K. V., Ferguson, R. B., & Turnock, A. C. 1972: Zoned plagioclases from Elbow Lake, Manitoba. I. Comparative microprobe and optical analysis. Canad. Min. 11, 488-503.

Vance, J. A. 1962: Zoning in igneous plagioclase: normal and oscillatory zoning. Am. Jour. Sci. 260, 746-760.

Wass, S. Y. 1973: The origin and petrogenetic significance of hour-glass zoning in titaniferous clinopyroxenes. Min. Mag. 39, 133-144.

Wiebe, R. A. 1968: Plagioclase stratigraphy: a record of magmatic conditions and events in a granite stock. Am. Jour. Sci. 266, 690-703.

TABLE 1

EXPERIMENTAL RUN CONDITIONS

Zone	Temp. °C	Pressure Kb	Time Hrs	Average Composition An wt. %	Range of Composition An wt. %	Average Growth Rate μ/hour
Run 65, An 30, 5.0 wt. % H_2O, T_L (initial) ~ 1090°C						
Melt	1200	6.1	17	--	-----	---
1	1050	5.3	24	61	59-62	1.3
2	1000	5.2	24	56	51-57	2.6
3	950	5.1	49	48	44-50	0.8
4	900	5.0	47	39	35-41	0.5
5	850	4.9	73	28	26-30	0.3
Glass	---	---	--	8	-----	---
Run 68, An 50, 10.0 wt. % H_2O, T_L ~ 1100°C						
Melt	1200	6.1	17	--	-----	---
1	1050	5.3	24	91	-----	2.5
2	1000	5.2	24	84	82-89	4.7
3	950	5.1	49	79	74-82	0.9
4	900	5.0	47	68	64-70	0.5
5	850	4.9	73	53	-----	0.4
Glass	---	---	--	13	-----	---
Run 74, An 40, 9.5 wt. % H_2O, T_L ~ 1040°C						
Melt	1100	6.2	24	--	-----	---
1	950	5.0	48	72	-----	1.4
2	900	4.9	50	60	58-63	0.6
3	850	4.8	71	48	45-49	0.3
4	800	4.7	73	30	-----	0.3
Glass	---	---	--	8	-----	---

Run 139, An 60, 7.1 wt. % H_2O

Melted at 1200°C for 7 hours, 5.3 Kb; dropped rapidly to 1150°C and then cooled at 4°C/hr to 800°C, the pressure decreased steadily with temperature from 5.3 to 4.7 Kb.

Run 391, An 40, 5.0 wt. % H_2O

Melted at 1200°C for 15.5 hours, 5.9 Kb; dropped rapidly to 1153°C and then cooled at 129°C/hr to 860°C, the pressure decreased steadily with temperature from 5.8 Kb at 1153°C to 4.7 Kb at 860°C.

TABLE I (cont.)

Run 618, An_{37} Ab45 Or18, 10.0 wt. % H_2O

Melted at 1100°C for 20 hours, 5.7 Kb; dropped rapidly to 1000°C and then cooled at 2°C/hr. to 500°C, the pressure decreased steadily with temperature from 5.5 Kb at 1000°C to 3.4 Kb at 500°C.

TABLE 2

CHEMICAL ANALYSES

Wt. %	M-714	M-736	M-229	M-513
SiO_2	51.46	61.77	66.93	68.44
TiO_2	1.08	0.60	0.40	0.50
Al_2O_3	20.73	14.42	14.78	15.59
Fe_2O_3	2.41	3.73	2.21	2.97
FeO	6.30	0.80	0.40	----
MnO	0.17	0.09	0.08	0.06
MgO	3.55	1.60	0.95	0.64
CaO	10.02	6.67	2.75	3.08
Na_2O	3.43	3.47	3.65	3.78
K_2O	0.81	3.67	3.83	3.39
P_2O_5	0.26	0.25	0.16	0.24
H_2O (total)	0.58	1.18	3.91	0.97
S	----	0.01	----	----
Total	100.80	98.26	100.05	99.66

NORMS
(Weight Percent)

Q	0.64	15.53	24.15	26.53
or	4.79	21.69	22.63	20.03
ab	29.02	29.36	30.89	31.99
an	38.78	12.93	12.63	13.87
di	7.76	8.59	0.05	-----
wo	-----	3.19	-----	-----
hy	13.12	-----	2.34	1.59
ol	-----	-----	-----	-----
hm	-----	2.95	1.94	2.97

TABLE 2 (cont.)

	NORMS (Weight Percent)			
mt	3.49	1.13	0.39	-----
il	2.05	1.14	0.76	0.13
ru	-----	-----	-----	0.43
ap	0.57	0.55	0.35	0.52
C	-----	-----	-----	0.62
Total	100.22	97.07	96.14	98.69

TABLE 3

MICROSCOPIC DATA

Sample	Extinction off (001) or (010) (Schuster's Method)	Composition (Schuster's Method)	Composition (Microprobe)
M-714			
Zone 1	-33°	An 91	An 88 to An 90.5
Zone 2	-26°	An 83	An 77 to An 81
Zone 3	-14° to -18°	An 66 to An 70	An 64 to An 71
Zone 4	- 9°	An 53	An 49 to An 54
M-513			
Zone 1	-31°	An 66	An 64 to An 65
Zone 2	-15° to -25°	An 48 to An 57	An 51 to An 59
Zone 3	- 3° to - 8°	An 39 to An 42	An 36 to An 43

TABLE 4

STATISTICAL ANALYSIS

	Traverse T-1 An % between 48 and 76 μm	Traverse T-2 An % between 30 and 54 μm	Traverse T-4 An % between 42 and 64 μm	Traverse T-5 An % between 50 and 74 μm
	36.6	36.8	36.7	37.2
	36.9	37.2	37.5	36.1
	37.3	36.3	37.1	37.2
Zone 1	33.8	33.0	38.1	37.0
	36.8	37.8	35.5	36.5
Zone 2	35.2	34.8	37.3	35.1
	36.4	36.9	37.0	37.9
	38.4	37.9	37.2	36.7
	36.3	35.5	34.8	37.3
	34.3	33.6	32.8	37.0
	32.8	33.0	36.8	34.5
Zone 3	31.7	36.1	36.7	36.6
	34.8	35.6		36.7
	36.5			
	34.0			
$\bar{x}$	35.45	35.73	36.46	36.60
s	1.85	1.70	1.45	0.92

$\bar{x}$ for total population = 36.03
s for total population = 1.57

Standard Deviation or Z Scores

Zone 1	-0.89	-1.61	-0.66	-1.63
Zone 2	-0.14	-0.55	-0.37	0.11
Zone 3	-2.03	-1.61	-2.52	-2.28

$$z = \frac{x - u}{s}$$

where x = An % at Zone 1, 2, 3,
u = mean of total population of each traverse, and
s = standard deviation of total population of each traverse.

t Test

Traverse		Zone 1	Zone 2	Zone 3
T-1		33.8	35.2	31.7
T-2		33.0	34.8	33.0
T-4		35.5	37.0	32.8
T-5		35.1	36.7	34.5
	$\bar{x}$	34.35	35.93	33.00
	s	1.16	1.09	1.15
	t	-2.13	-0.13	-3.84

TABLE 4 (cont.)

$$t = \frac{\bar{x} - u}{s/\sqrt{n}}$$

where $\bar{x}$ = mean for zones 1, 2, and 3,
u = mean for total population of traverses T-1, T-2, T-4, and T-5
s = standard deviation for total population of traverses T-1, T-2, T-4, and T-5, and
n = sample size (4, in present study).

Sign Test - Zone 1

$H_o: u_{in} = u_{zone\ 1}$ $\quad P[+] = .5$ $\quad H_o: u_{zone\ 1} = u_{out}$

$H_1: u_{in} > u_{zone\ 1}$ $\quad P[+] > .5$ $\quad H_1: u_{zone\ 1} < u_{out}$

In	-	Zone 1	=	Difference	Sign
37.3	-	33.8	=	3.5	+
36.3	-	33.0	=	3.3	+
38.1	-	35.5	=	2.6	+
36.5	-	35.1	=	1.4	+

Zone 1	-	Out	=	Difference	Sign
33.8	-	36.8	=	-3.0	-
33.0	-	37.8	=	-4.8	-
35.5	-	37.3	=	-1.8	-
35.1	-	37.9	=	-2.8	-

x = number of + signs

If H_o true:

$$P[x \geq 4] = \binom{4}{4} (.5)^4 (.5)^0 = .0625$$

$$P[x \leq 0] = \binom{4}{4} (.5)^4 (.5)^0 = .0625$$

H_o: signs of differences the same $P = .5$

H_1: signs of differences different $P \neq .5$

x = number of changes

$$P[x \leq 0] = \binom{4}{4} (.5)^4 (.5)^0 = .0625$$

Zones 2 and 3 yield the same results.

LIST OF FIGURES

discontinuous zoning superimposed on a normal zoning trend. Crossed polarizers.

Fig. 6. Photomicrograph of an oscillatory zoned plagioclase phenocryst in a holocrystalline latite (trachyandesite) porphyry from the San Juan Mountains, Colorado. Note the nearly homogeneous core enclosed by an outer region of discontinuous and oscillatory zoning with both reverse and normal trends. Crossed polarizers.

Fig. 7. Photomicrographs of plagioclase phenocrysts displaying rhythmic oscillations in (A) a hypocrystalline trachyte porphyry from near the Hoover Dam, Arizona and (B) in a hyprocrystalline basalt porphyry from Chile. Crossed polarizers.

Fig. 8. Photomicrographs displaying rhythmic oscillations in a hypocrystalline basalt porphyry from Chile. (A) Shows number, location, and extent of microprobe traverses. (B-D) Show the compositional detail for microprobe traverses T-1, T-5, and T-7. Crossed polarizers.

Fig. 9. Experimentally grown plagioclase crystal showing fine-scale, oscillatory zoning. See Table 1, run 139 for experimental data. Crossed polarizers.

Fig. 10. Experimentally grown plagioclase crystals showing sector zoning. (A) Microprobe traverse showing relatively symmetrical normal zoning trends. (B) Shows a normal zoning trend in the (001) direction. (C) Photomicrograph showing sector zoned crystal and location of microprobe traverse shown in (D). See Table 1, run 618 for experimental data. Crossed polarizers.

Fig. 11. Photomicrographs of discontinuously zoned plagioclase crystals used in the optical comparison of zone compositions using Schuster's method. (A) M-714A, (B) M-513. Data and compositional comparisons are shown in Table 3. Crossed polarizers.

Fig. 12. Four 2 μm step scan traverses with separate 6 element spot analyses superimposed (solid black circles). Figures A (M-600) and B (M-714A, Table 2) represent naturally occurring plagioclase phenocrysts, while C (run 68, Table 1) and D (run 139, Table 1) represent experimentally grown plagioclase phenocrysts. In each case note the close correlation between the 3 element and 2 μm step scan traverses and the separate 6 element spot analyses.

Fig. 13. Shown are four separate microprobe traverses (M-600, Fig. 8A) selected to test statistically the significance of the very small, but sharp, microprobe compositional oscillations. On each traverse microscopically correlatable minor oscillations are numbered 1, 2, and 3 (solid and dashed lines).

NASA National Aeronautics and Space Administration

Lyndon B. Johnson Space Center
Houston, Texas 77058

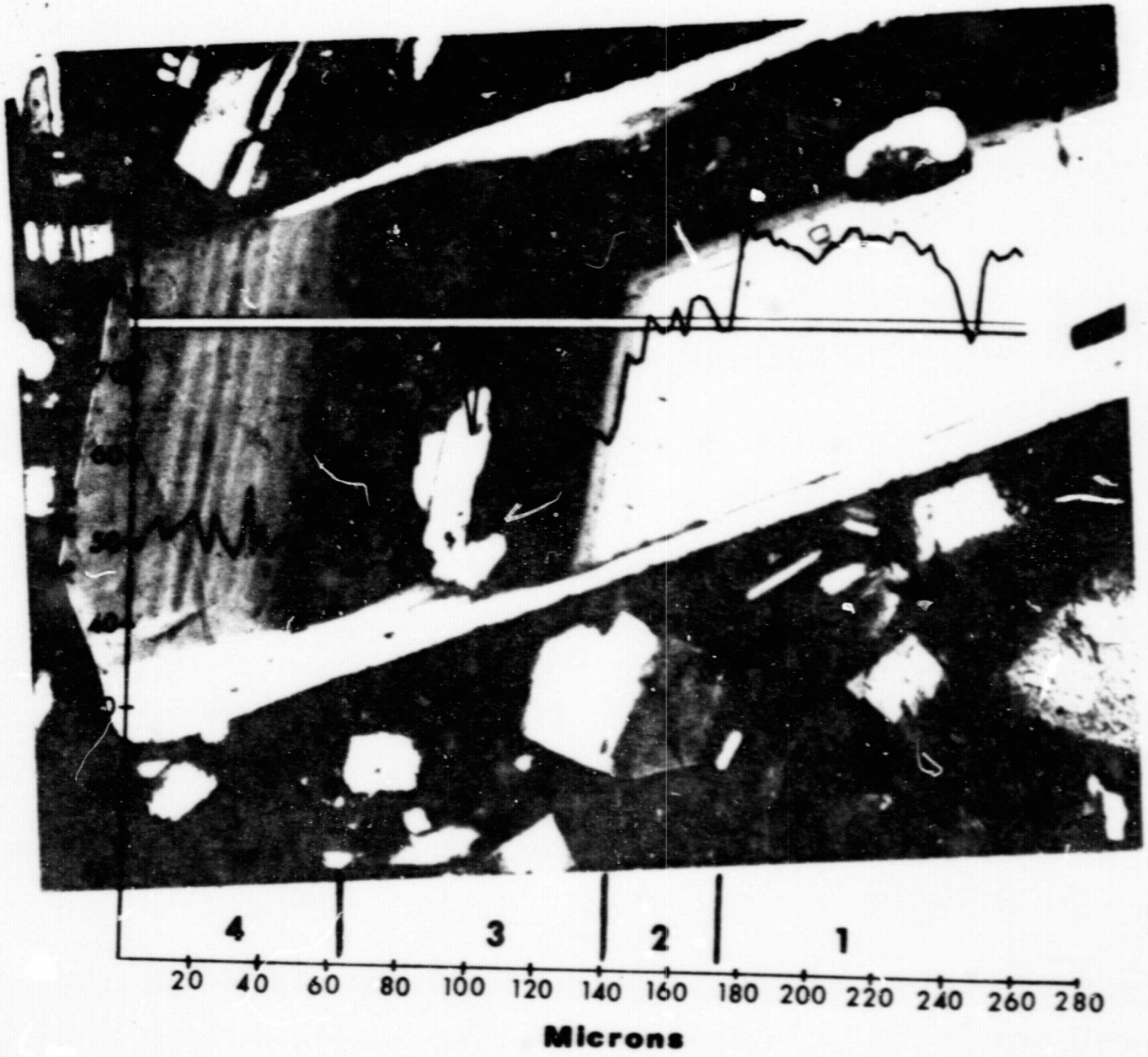

Smith & Lofgren
Fig. 1

M-714A,T-2

ORIGINAL PAGE
BLACK AND WHITE PHOTOGRAPH

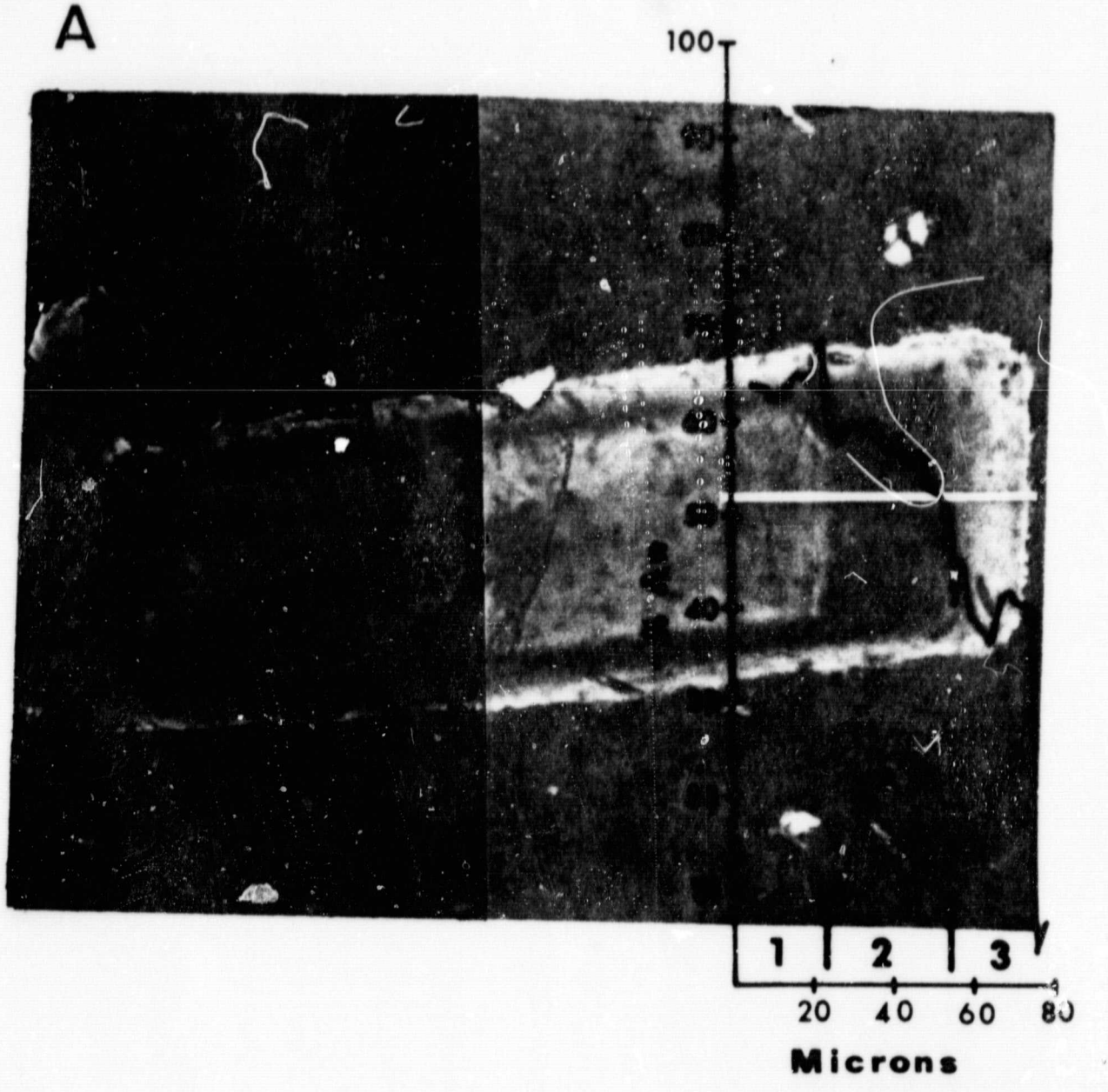

Smith & Lofgren
Fig. 2A

ORIGINAL PAGE
BLACK AND WHITE PHOTOGRAPH

Smith & Lofgren
Fig. 2B

Smith & Lofgren
Fig. 3

ORIGINAL PAGE
BLACK AND WHITE PHOTOGRAPH

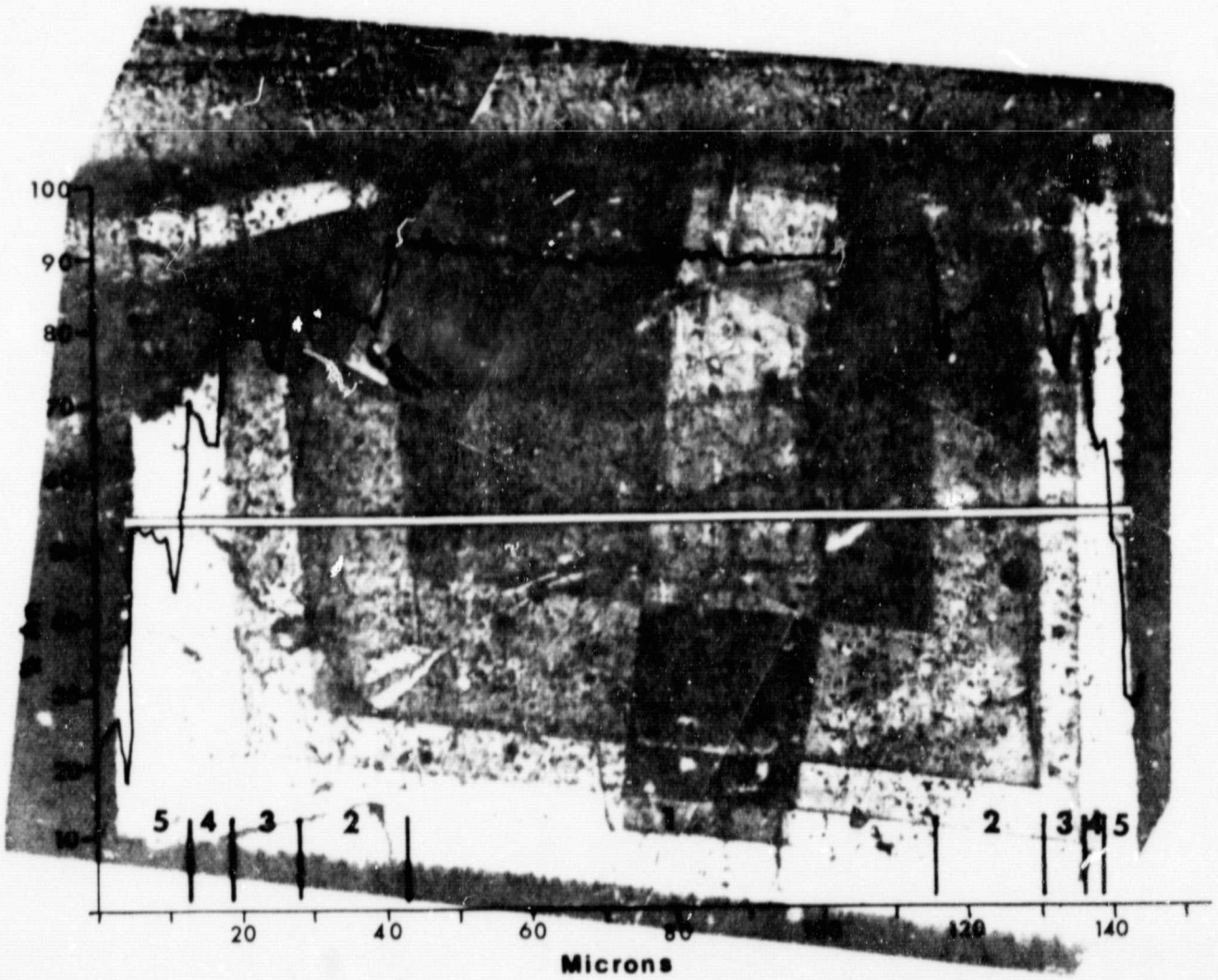

#68, T-1

NASA
National Aeronautics and Space Administration

Lyndon B. Johnson Space Center
Houston, Texas 77058

ORIGINAL PAGE
BLACK AND WHITE PHOTOGRAPH

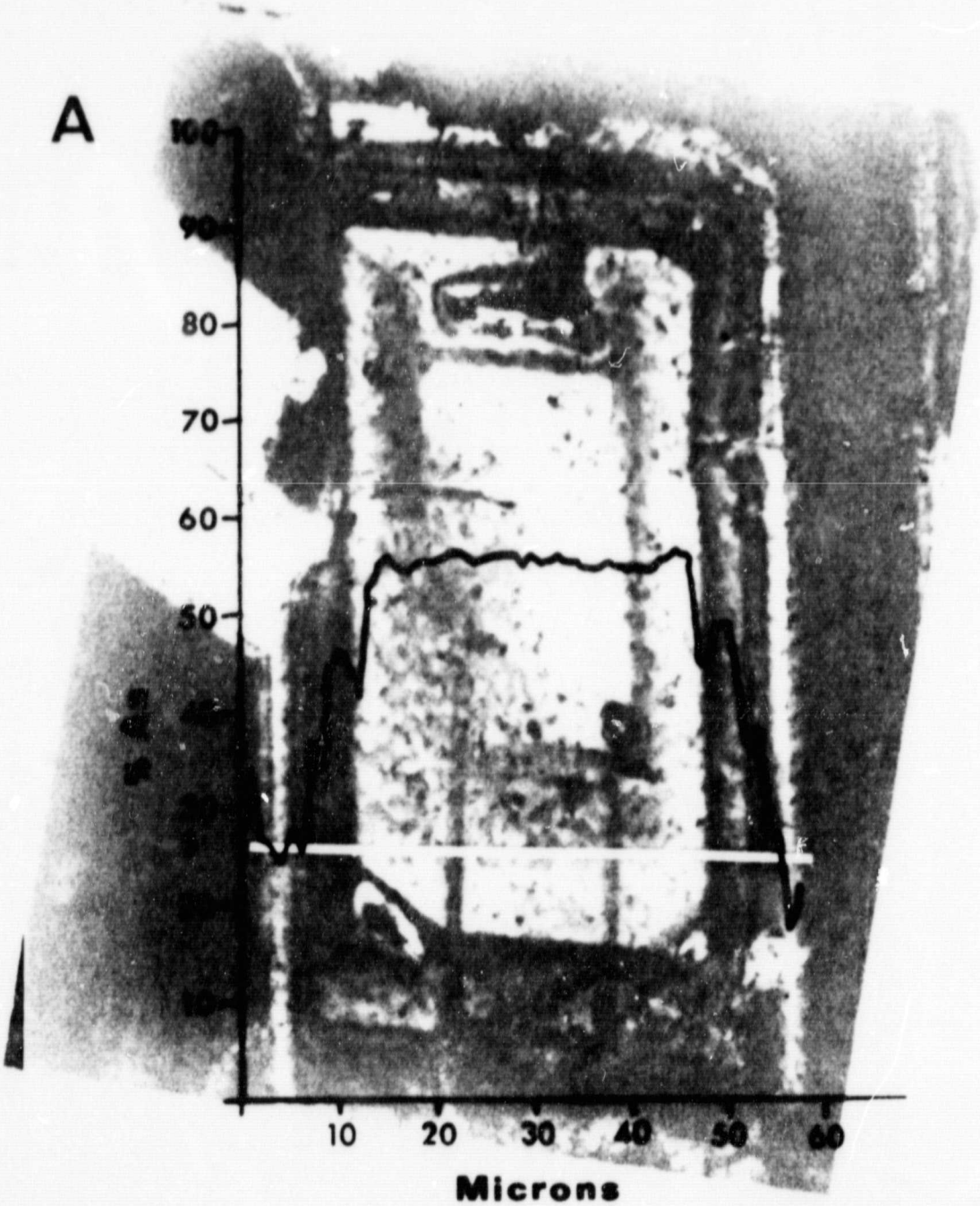

Smith & Lofgren
Fig. 4A

ORIGINAL PAGE
BLACK AND WHITE PHOTOGRAPH

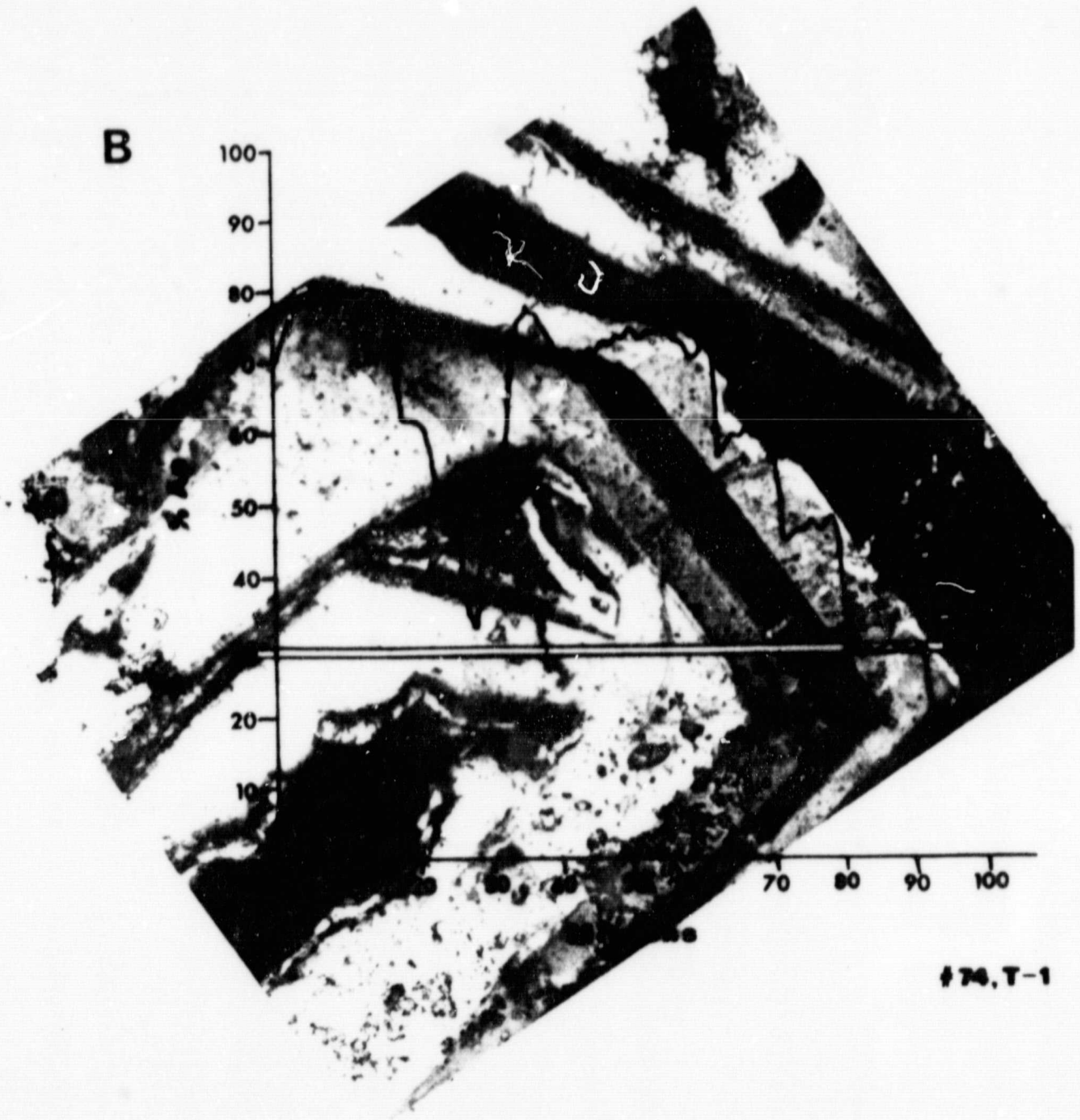

NASA National Aeronautics and Space Administration

Lyndon B. Johnson Space Center
Houston, Texas 77058

Smith & Lofgren
Fig. 4B

NASA National Aeronautics and Space Administration

Lyndon B. Johnson Space Center
Houston, Texas 77058

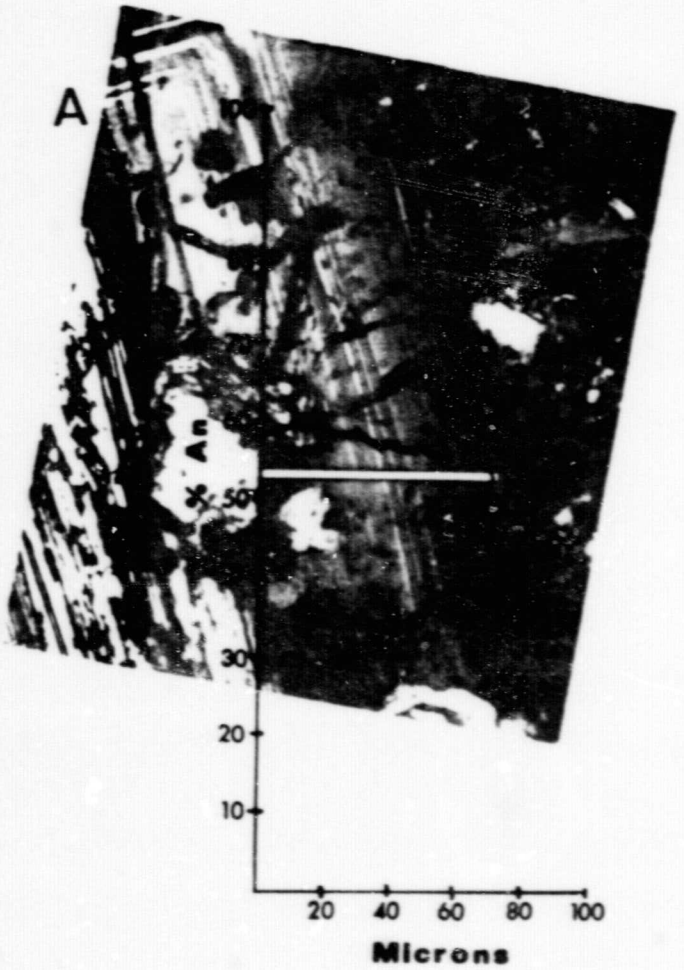

M-598,T-1

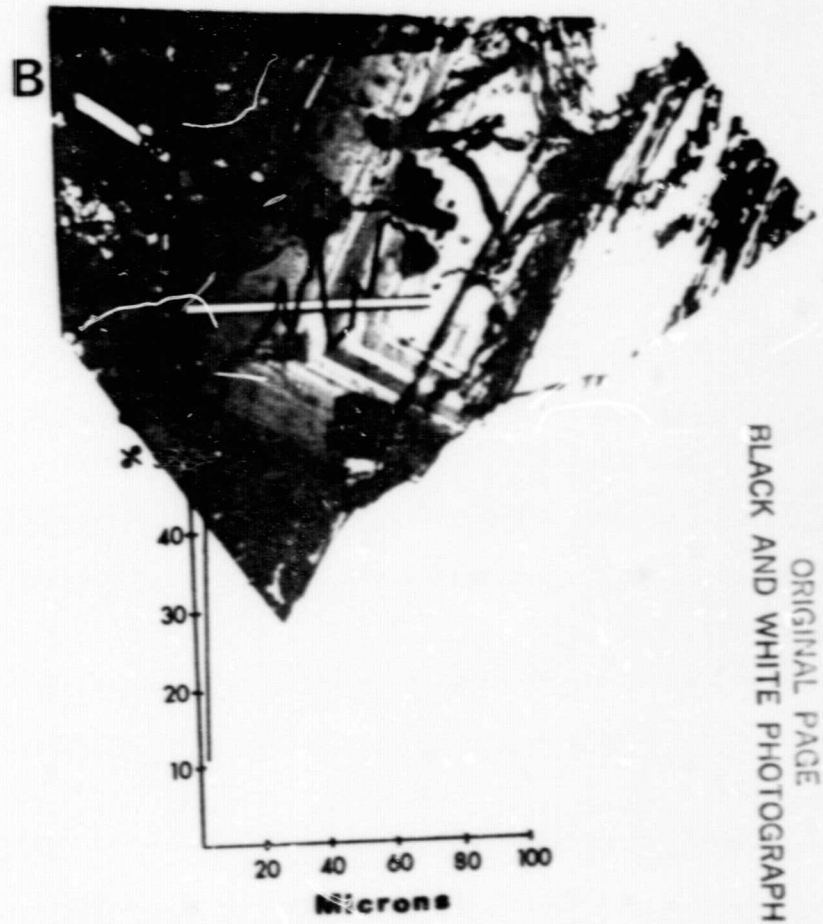

M-598,T-6

Smith & Lofgren
Fig. 5A, B

ORIGINAL PAGE
BLACK AND WHITE PHOTOGRAPH

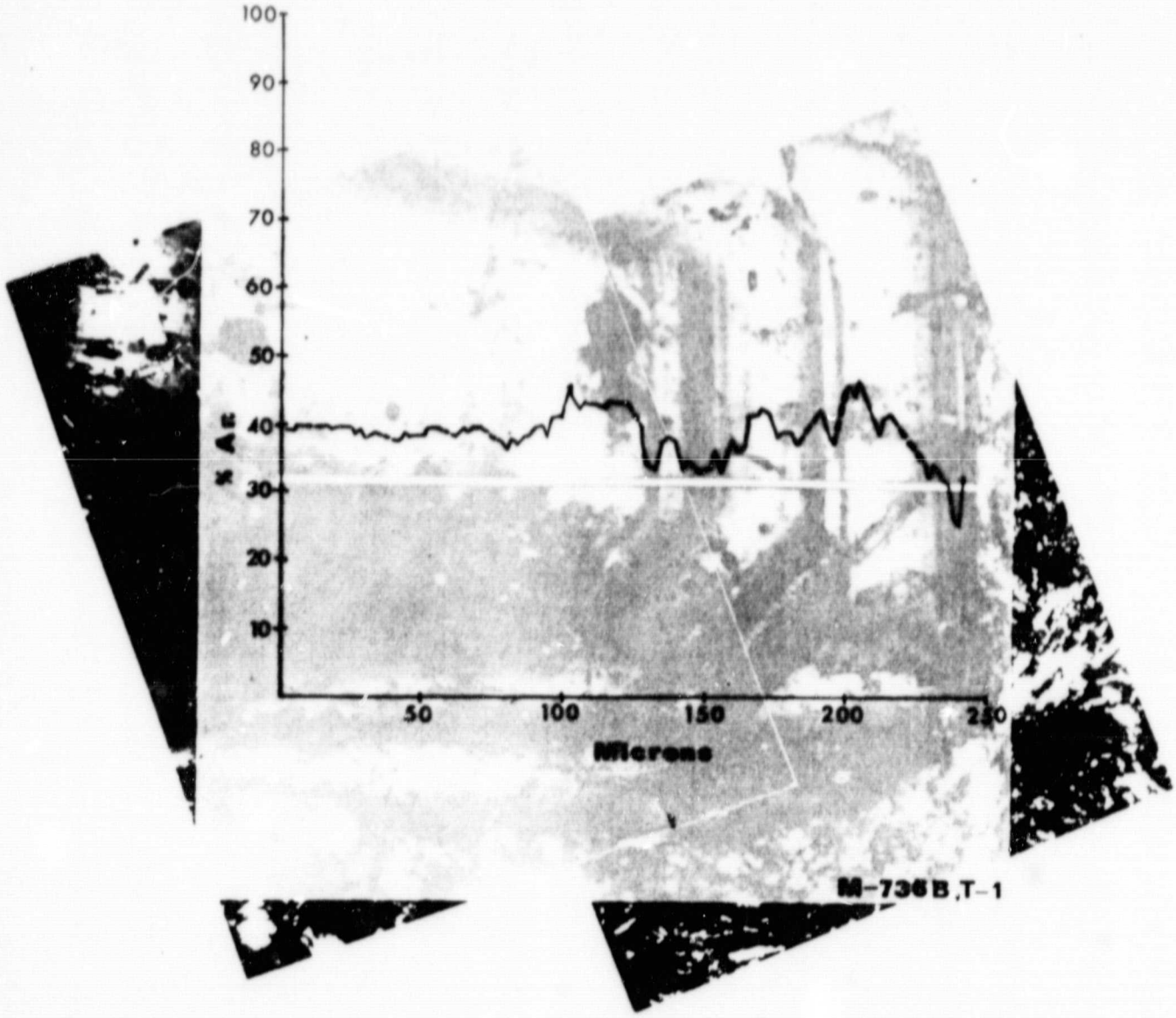

NASA National Aeronautics and Space Administration

Lyndon B. Johnson Space Center
Houston, Texas 77058

Smith & Lofgren
Fig. 6

ORIGINAL PAGE
BLACK AND WHITE PHOTOGRAPH

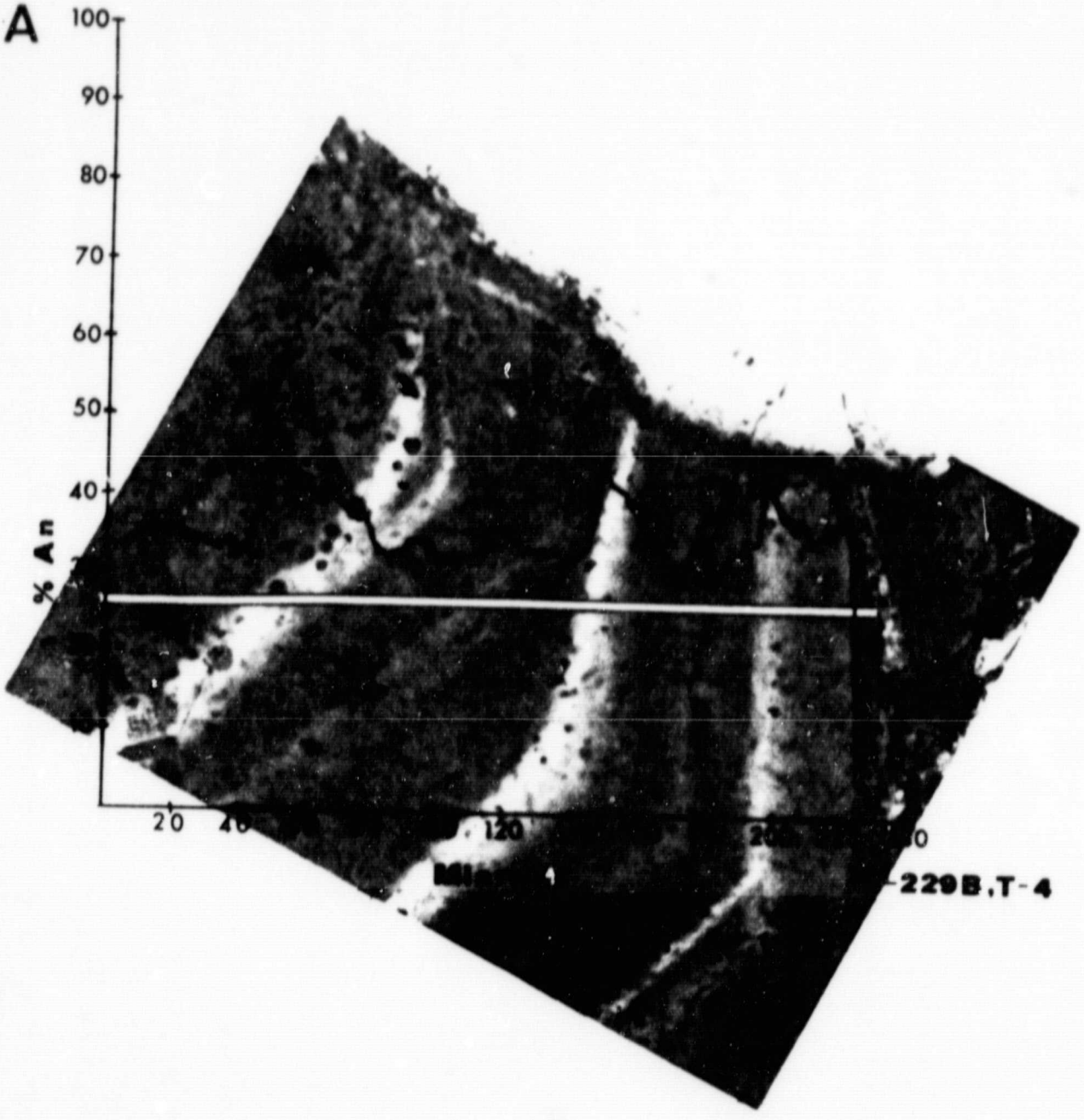

Smith & Lofgren
Fig. 7A

NASA National Aeronautics and Space Administration

Lyndon B. Johnson Space Center
Houston, Texas 77058

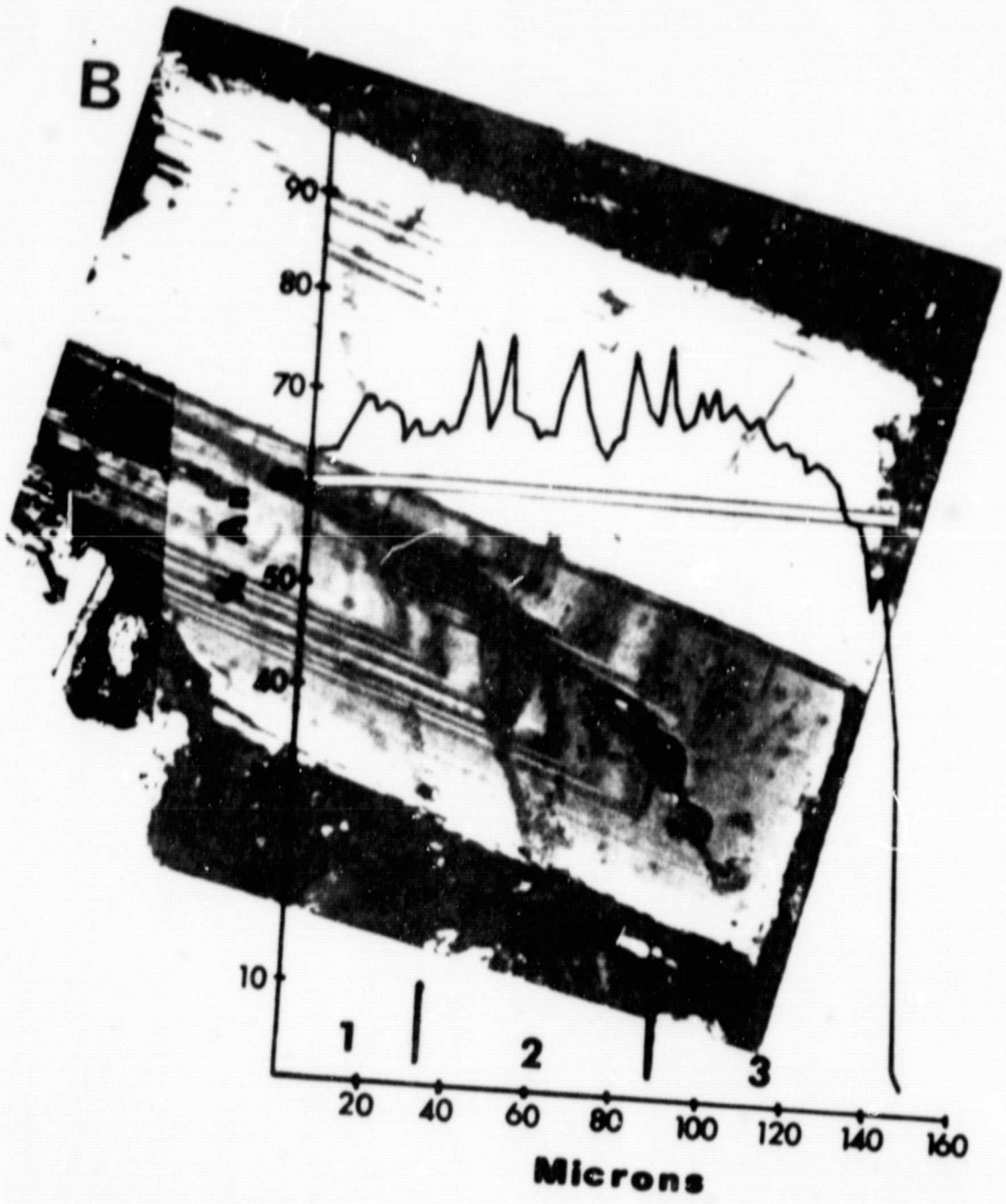

Smith & Lofgren
Fig. 7B

M-598,T-3

ORIGINAL PAGE
BLACK AND WHITE PHOTOGRAPH

Smith & Lofgren
Fig. 8A

NASA
National Aeronautics and Space Administration

Lyndon B. Johnson Space Center
Houston, Texas 77058

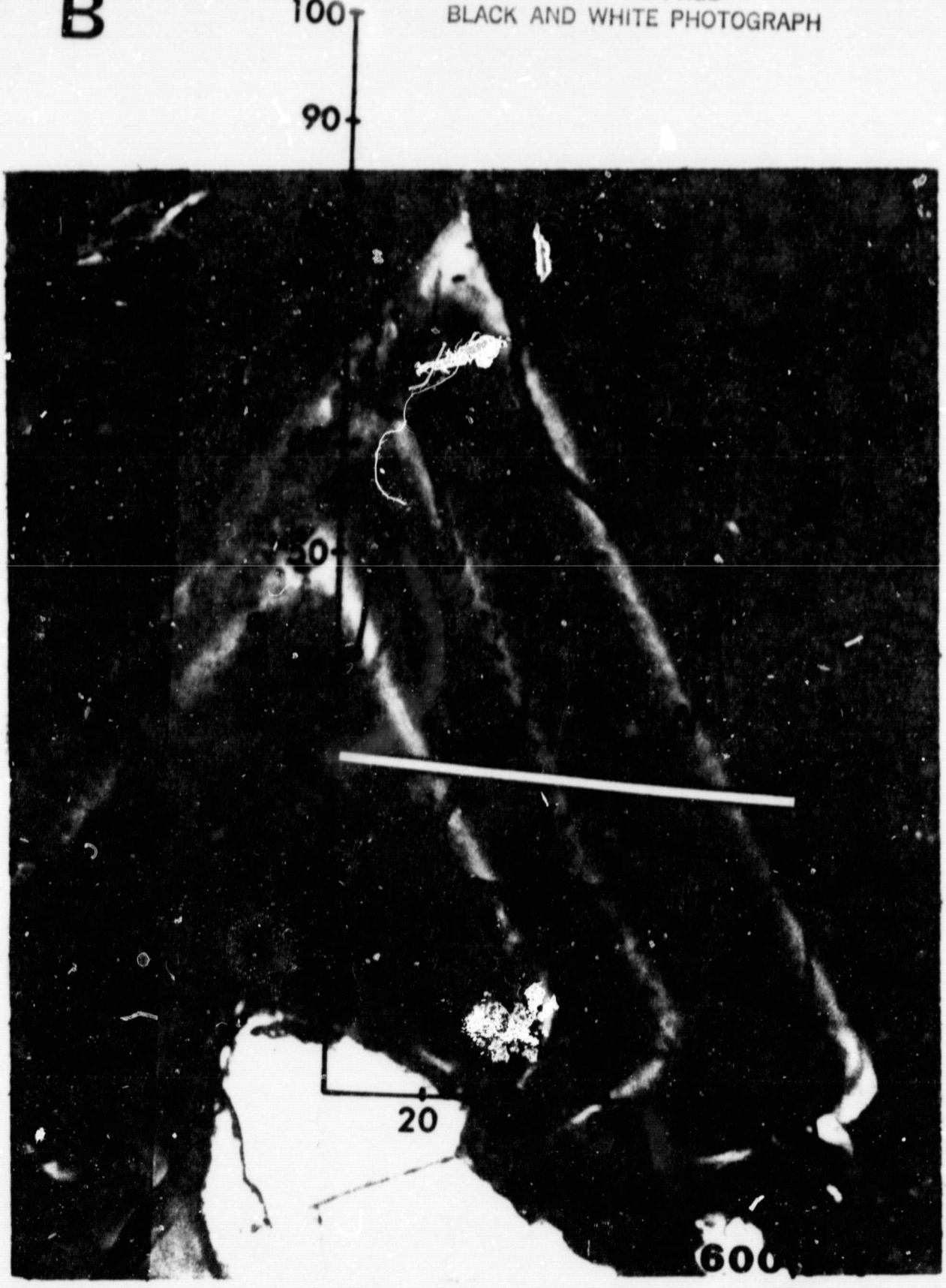

Smith & Lofgren
Fig. 8B

ORIGINAL PAGE
BLACK AND WHITE PHOTOGRAPH

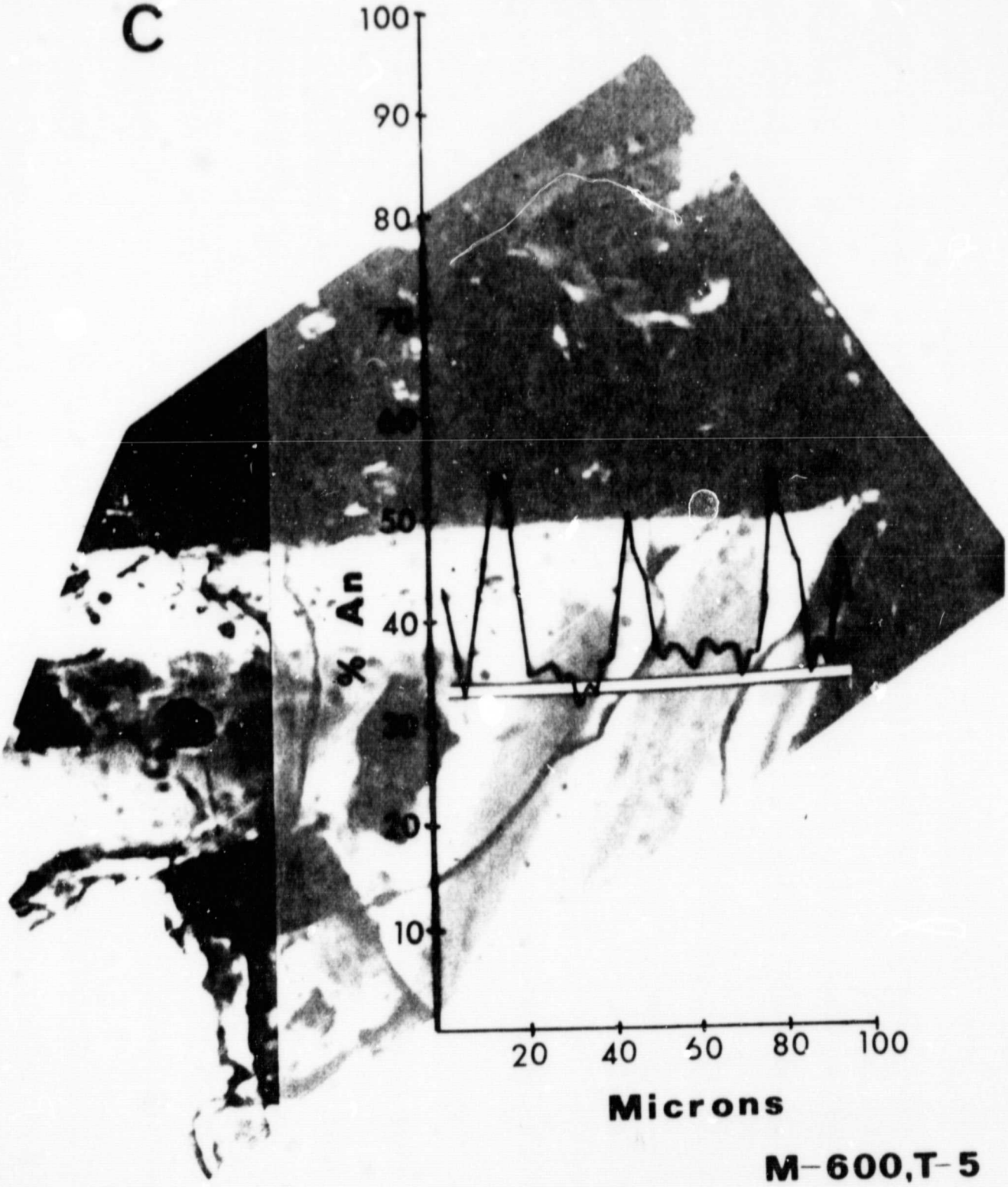

NASA National Aeronautics and Space Administration

Lyndon B. Johnson Space Center
Houston, Texas 77058

Smith & Lofgren
Fig. 8C

ORIGINAL PAGE
BLACK AND WHITE PHOTOGRAPH

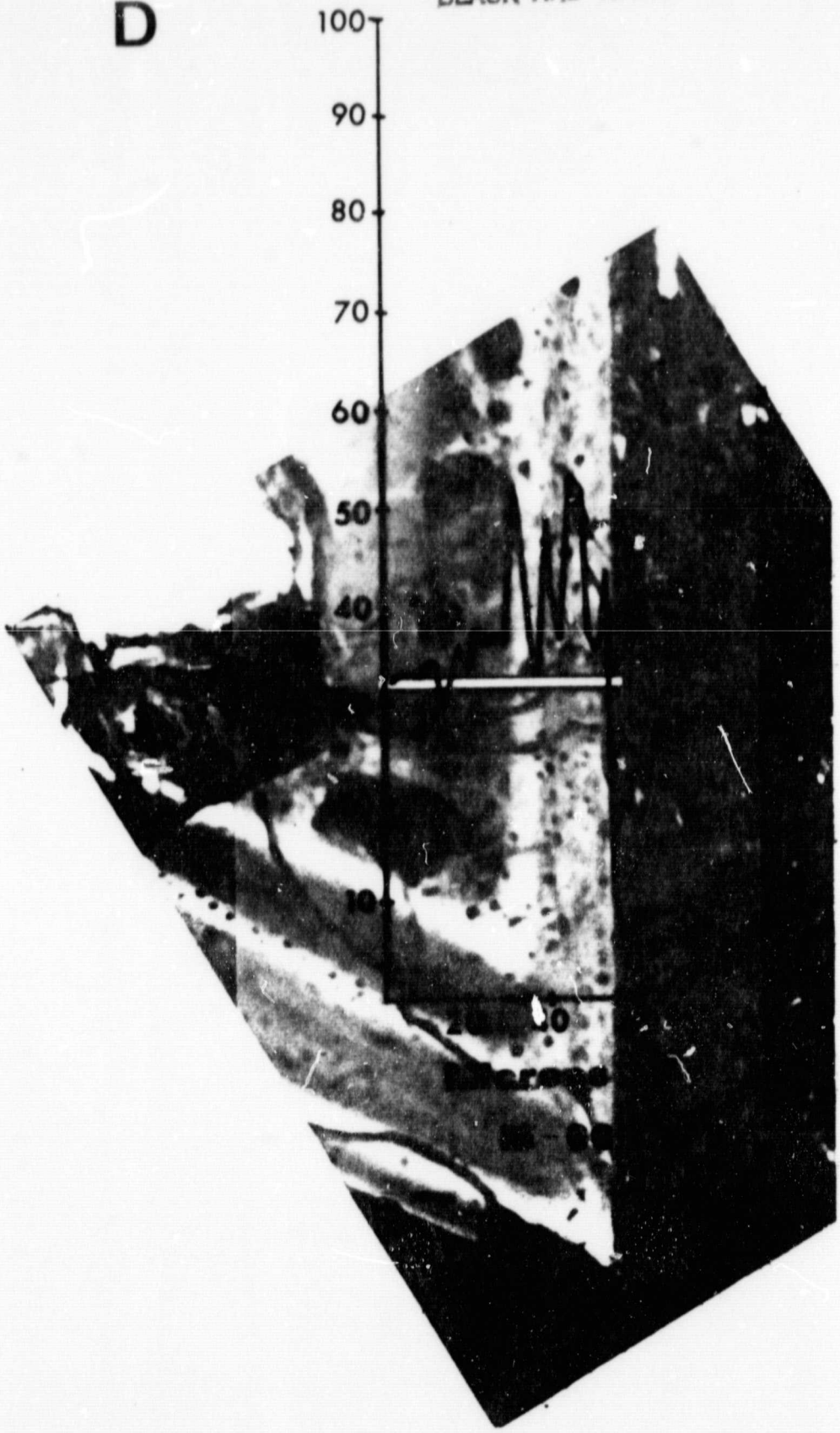

NASA National Aeronautics and Space Administration

Lyndon B. Johnson Space Center
Houston, Texas 77058

Smith & Lofgren
Fig. 8D

ORIGINAL PAGE
BLACK AND WHITE PHOTOGRAPH

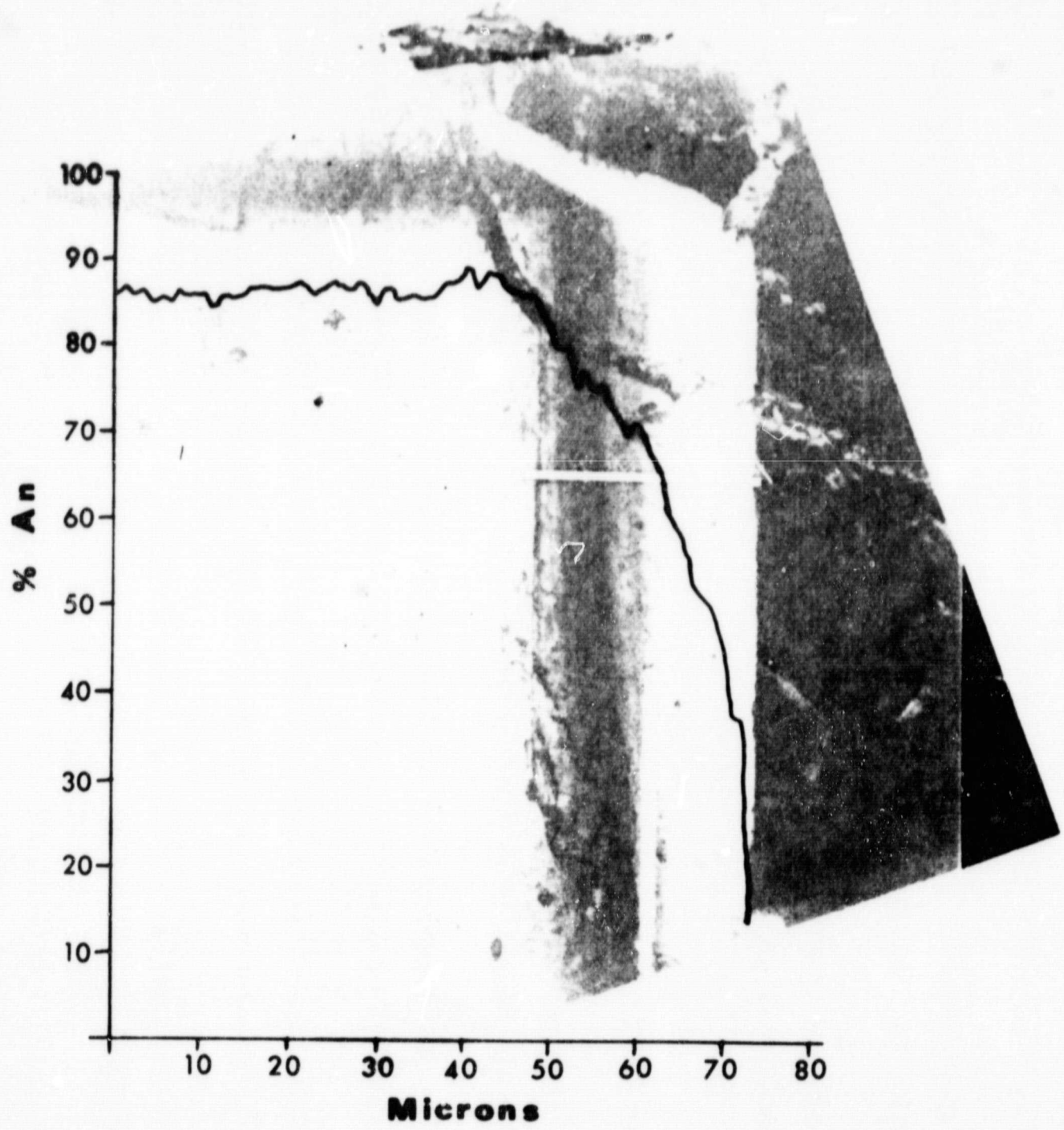

NASA National Aeronautics and Space Administration

Lyndon B. Johnson Space Center
Houston, Texas 77058

Smith & Lofgren
Fig. 9

ORIGINAL PAGE
BLACK AND WHITE PHOTOGRAPH

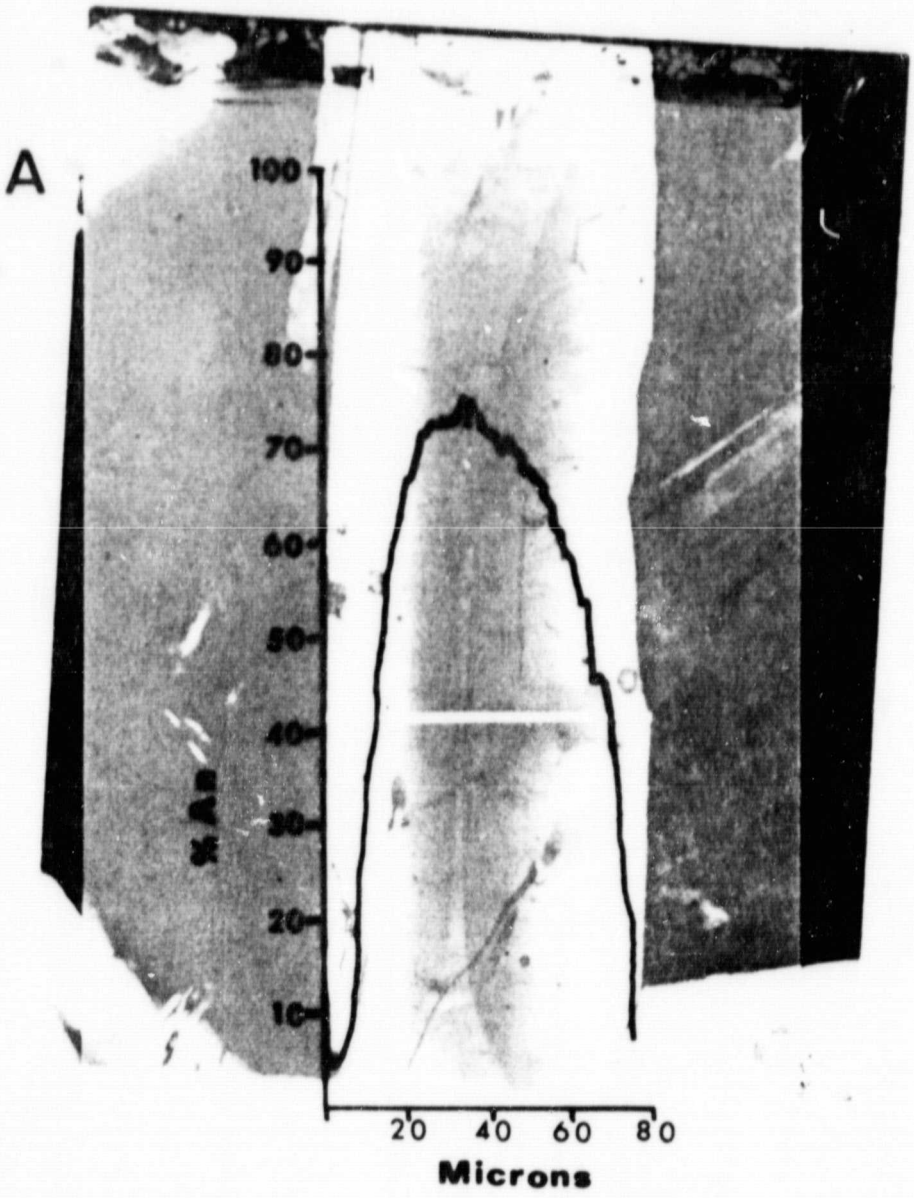

Smith & Lofgren
Fig. 10A

ORIGINAL PAGE
BLACK AND WHITE PHOTOGRAPH

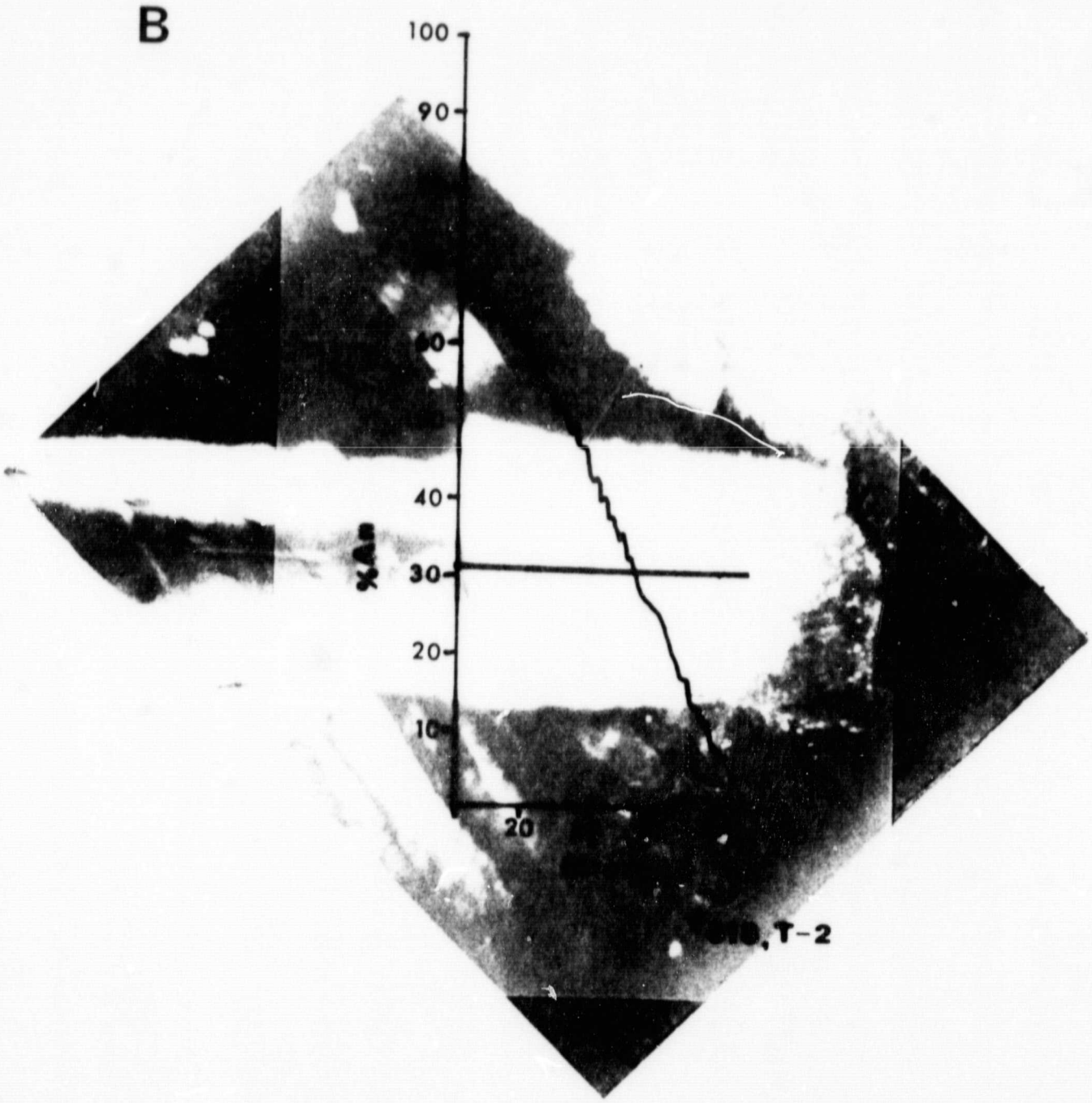

Smith & Lofgren
Fig. 10B

NASA
National Aeronautics and Space Administration

Lyndon B. Johnson Space Center
Houston, Texas 77058

C

Smith & Lofgren
Fig. 10C

Smith & Lofgren
Fig. 10D

ORIGINAL PAGE
BLACK AND WHITE PHOTOGRAPH

A

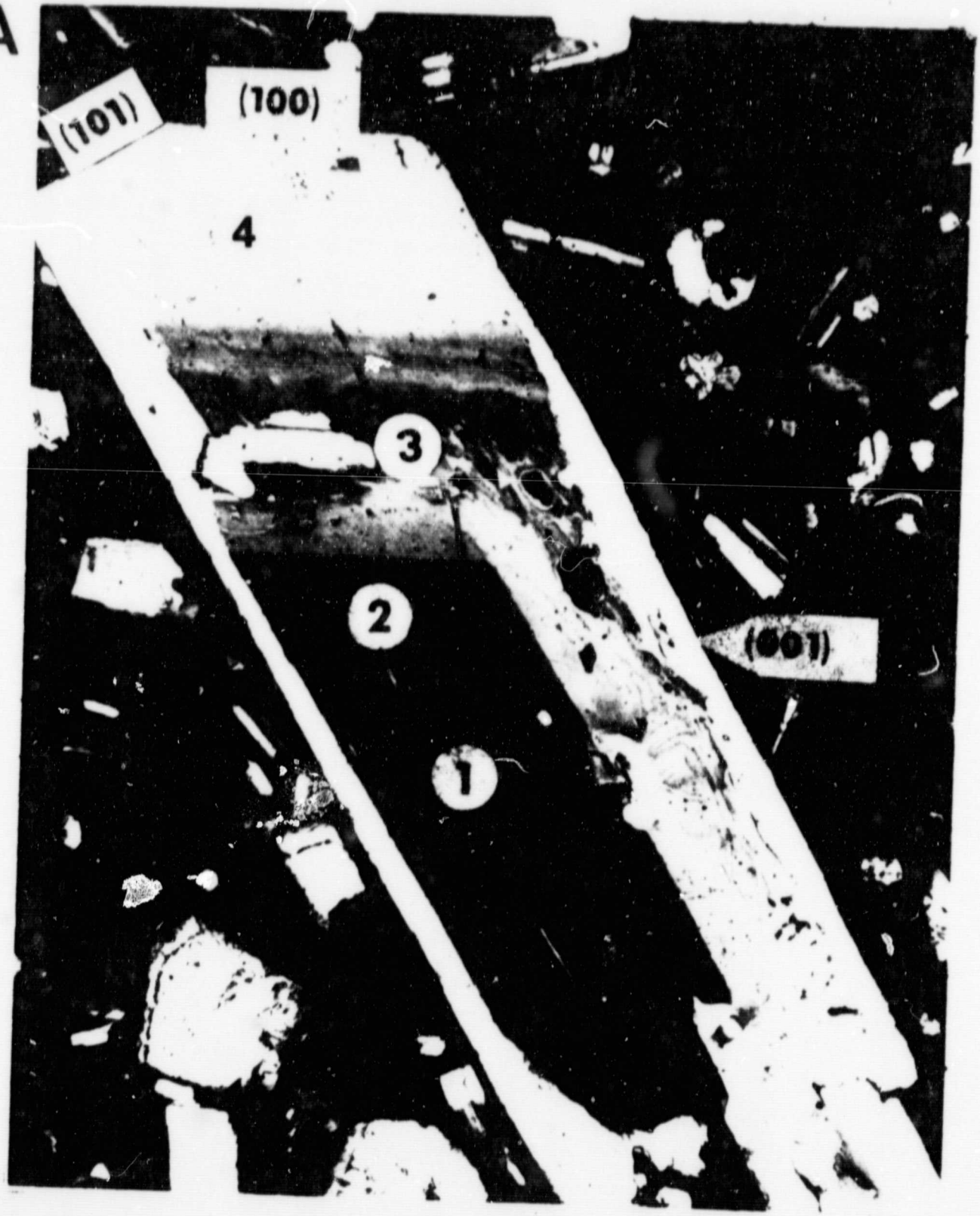

Smith & Lofgren
Fig. 11A

NASA National Aeronautics and Space Administration

Lyndon B. Johnson Space Center
Houston, Texas 77058

NASA National Aeronautics and Space Administration

Lyndon B. Johnson Space Center
Houston, Texas 77058

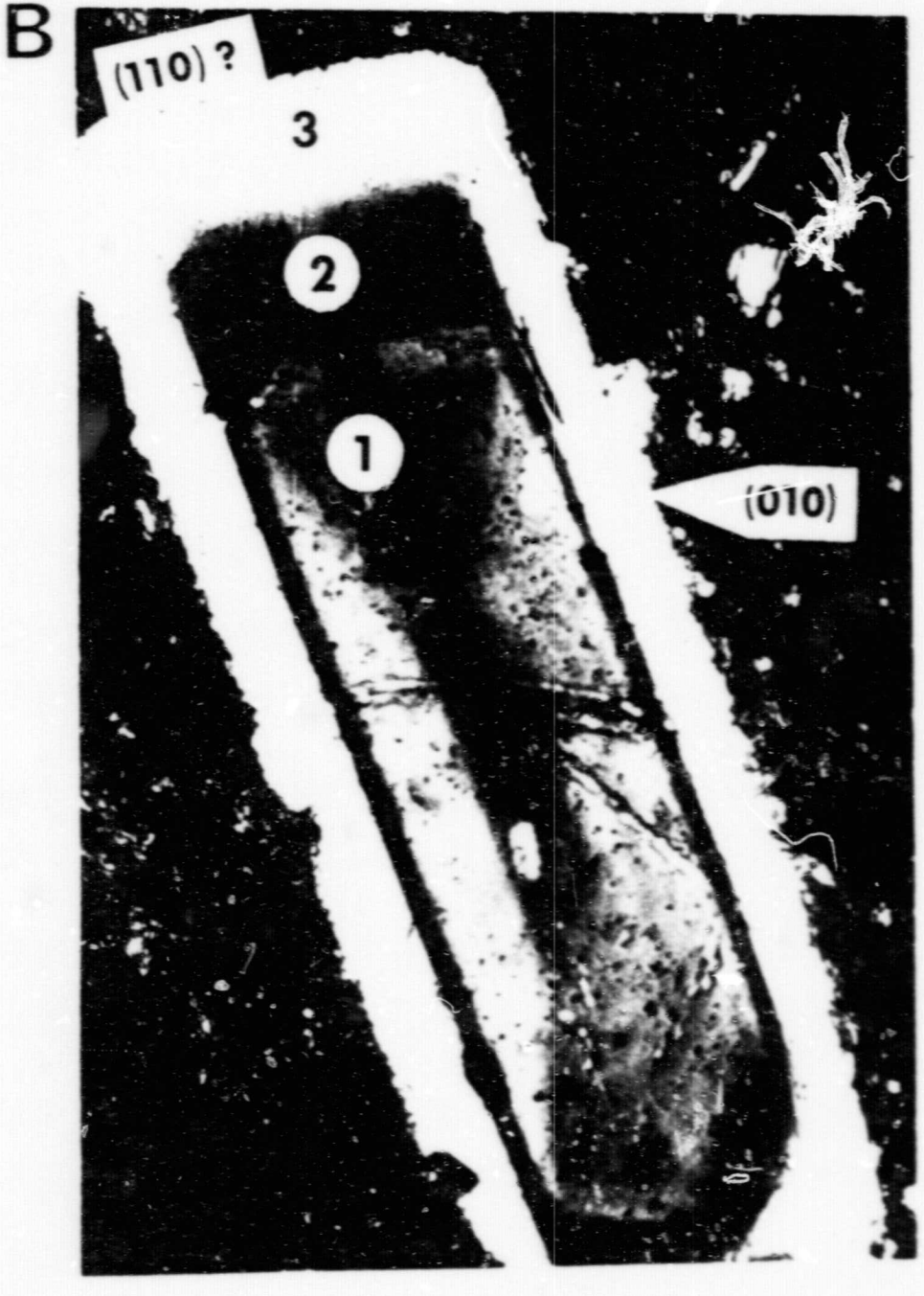

Smith & Lofgren
Fig. 11B

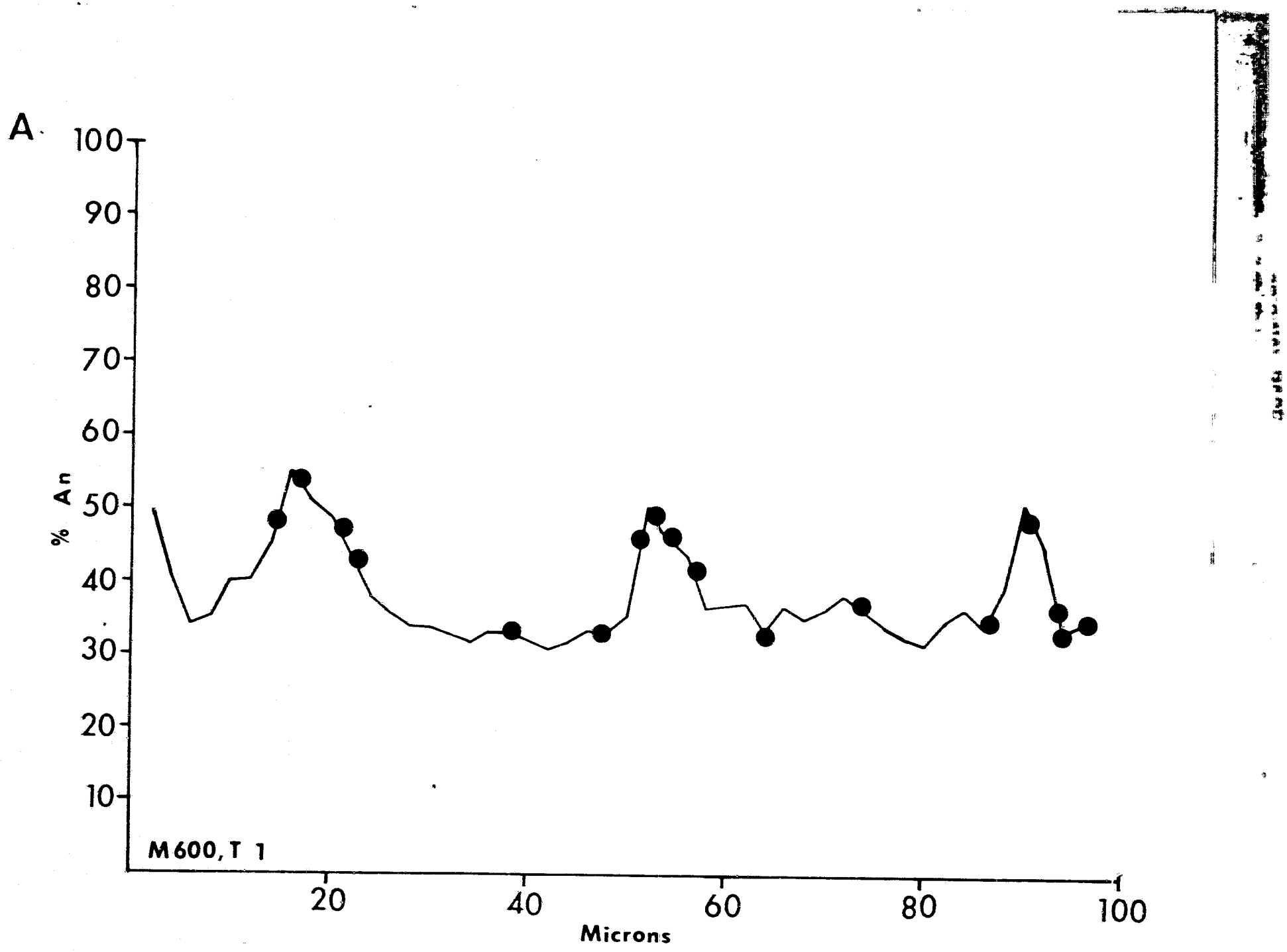

Smith & Lofgren
Fig. 12A

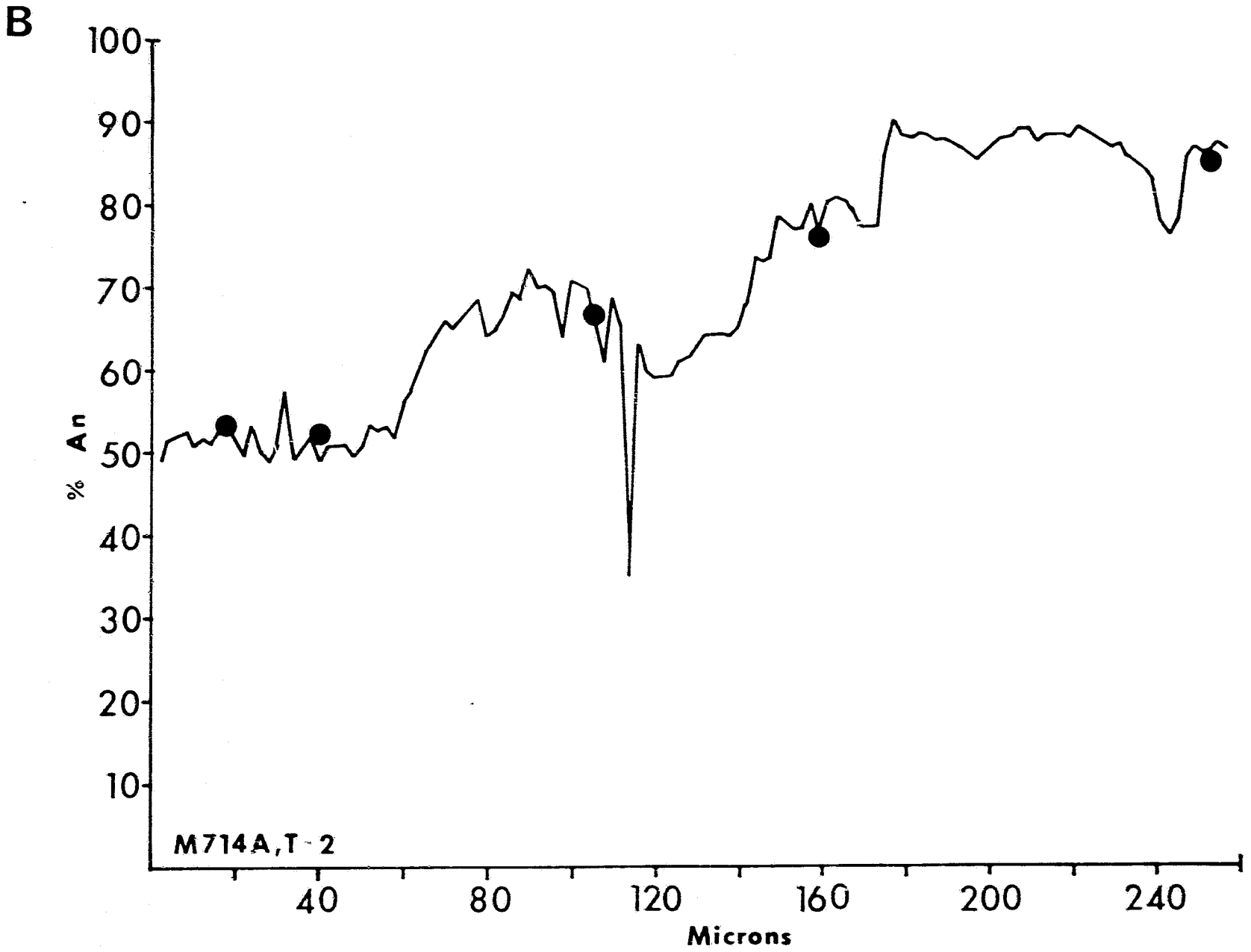

Smith & Lofgren
Fig. 12B

C

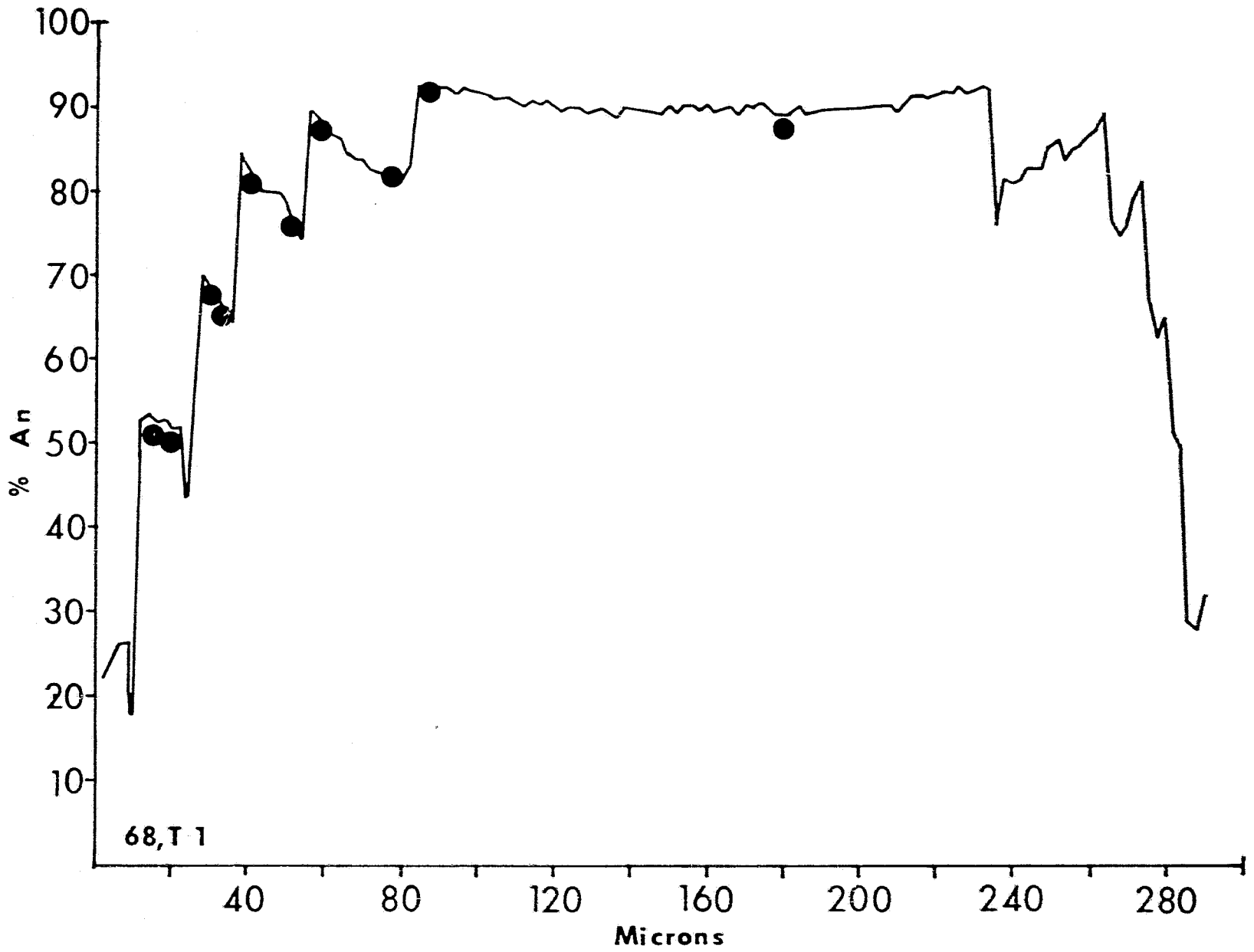

Smith & Lofgren
Fig. 12C

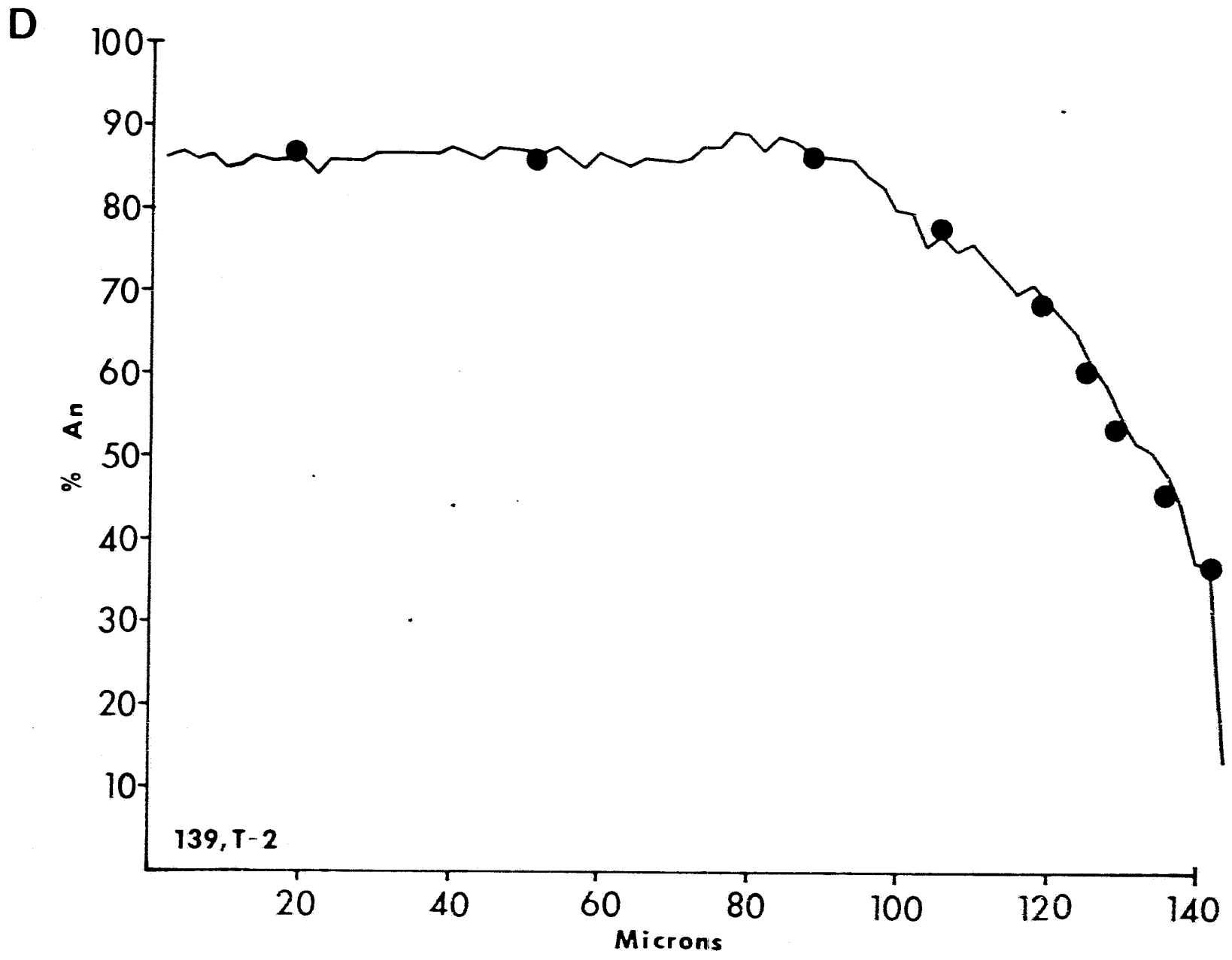

Smith & Lofgren
Fig. 12D

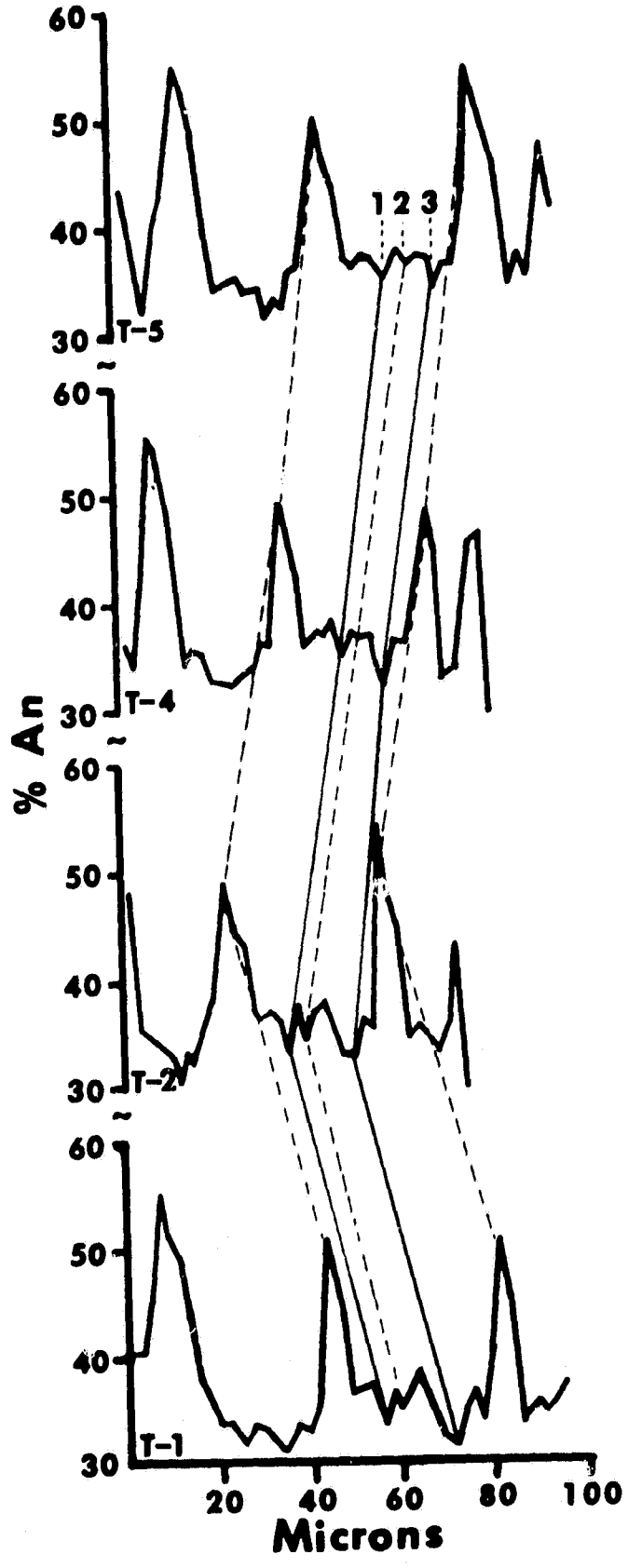

Smith & Lofgren
Fig. 13